

BT Worldsheet for Supersymmetric Gauge Theories*

Skuli Gudmundsson[†], Charles B. Thorn[‡], and Tuan A. Tran[§]

*Institute for Fundamental Theory
Department of Physics, University of Florida, Gainesville FL 32611
(November 2, 2018)*

Abstract

We extend the Bardakci-Thorn (BT) worldsheet formalism to supersymmetric non-abelian gauge theory. Our method covers the cases of $\mathcal{N} = 1, 2, 4$ extended supersymmetry. This task requires the introduction of spinor valued Grassmann variables on the worldsheet analogous to those of the supersymmetric formulation of superstring theory. As in the pure Yang-Mills case, the worldsheet formalism automatically generates the correct quartic vertices from the cubic vertices. We also discuss coupling renormalization to one loop order.

*This work was supported in part by the Department of Energy under Grant No. DE-FG02-97ER-41029.

[†]E-mail address: skulig@phys.ufl.edu

[‡]E-mail address: thorn@phys.ufl.edu

[§]E-mail address: tuan@phys.ufl.edu

1 Introduction

Last year Bardakci and one of us [1] proposed a method for mapping each individual planar Feynman diagram of the large N_c limit [2] of a matrix quantum field theory onto the evolution amplitude of a “topological” worldsheet dynamical system defined on a light-cone worldsheet [3–5]. The sum over all planar diagrams is then accomplished through the introduction of an Ising-like spin system on this same worldsheet, which is coupled to the target space worldsheet fields. This interacting system can be thought of as noninteracting string propagating on a highly non-trivial background represented by the Ising-like spins. The initial proposal was developed for $\text{Tr}\phi^3$ scalar field theory, but the formalism was soon extended to the case of pure Yang-Mills theory [6].

Extracting the physics of the large N_c limit of pure Yang-Mills theory is probably the most exciting potential application of this new formalism. It would be the zeroth order of a systematic expansion of QCD in powers of $1/N_c$, which would provide theoretical physics with an analytic understanding of the spectrum and structure of glueballs and, with the inclusion of quarks, that of other hadrons. A mean field method for capturing the nonperturbative physics of the worldsheet formalism has already been initiated [7]. If the idea of a quasi-perturbative gluon chain model of the quark confining flux tube [8, 9] is indeed viable, the BT worldsheet formalism should be the ideal setting for its development. This is because the stringy features of the theory are extracted directly from the perturbative diagrams.

However, in this article, we are interested in testing the BT formalism by extending it to theories for which a stringy description has been understood from other points of view. In particular, Maldacena [10] has proposed that the large N_c limit of $\mathcal{N} = 4$ supersymmetric Yang-Mills theory is equivalent to a noninteracting string theory on an $\text{AdS}_5 \times \text{S}_5$ background [10–12]. Unfortunately, calculations in this approach have generally been tractable only at large ’t Hooft coupling $N_c g_s^2 \rightarrow \infty$. Since the BT worldsheet is based on *weak* ’t Hooft coupling, it should provide complementary insight into the workings of Maldacena duality. Therefore, in this article we extend the formalism to include fermions and, in particular, our method covers the cases of supersymmetric gauge theories with $\mathcal{N} = 1, 2, 4$. Study of the $\mathcal{N} = 4$ case should then throw new light on the Maldacena conjecture. We note in passing two earlier works that share similar goals to ours but differ in method. The first [13] is an effort to abstract a covariant worldsheet formalism from the planar graphs of $\mathcal{N} = 4$ supersymmetric gauge theories. A more recent work on the pp-wave limit of $\text{AdS}_5 \times \text{S}_5$ has led to another intriguing interpolation between the strong and weak coupling regimes [14].

The worldsheet construction of Ref [1] exploits light-cone coordinates[¶]. On the light-cone x^+ is the quantum evolution parameter, and the Hamiltonian conjugate to this time is p^- . A massless on-shell particle thus has the “energy” $p^- = \mathbf{p}^2/2p^+$. The construction begins with the identification of a worldsheet system that reproduces the mixed representation (x^+, p^+, \mathbf{p}) of the propagator of a free massless scalar field [2]:

$$\exp\left\{-\tau \frac{\mathbf{p}^2}{2p^+}\right\} = \int DcDbD\mathbf{q} \exp\left\{-\int_0^T d\tau \int_0^{p^+} d\sigma \left[\frac{\mathbf{q}'^2}{2} - b'c'\right]\right\}. \quad (1)$$

Here the prime denotes $\partial/\partial\sigma$, and we are working with imaginary x^+ or real $\tau \equiv ix^+$. With lightcone parametrization the worldsheet is just a rectangle of width p^+ and length T . In the path integral the worldsheet fields include the target space field $\mathbf{q}(\sigma, \tau)$, with Dirichlet boundary conditions constrained by $\mathbf{q}(p^+, \tau) - \mathbf{q}(0, \tau) = \mathbf{p}$ the total transverse momentum of the system. The derivative of \mathbf{q} is the density of transverse momentum on a bit of worldsheet: that is $\mathbf{q}'d\sigma$ is the transverse momentum carried by the element $d\sigma$. The anticommuting ghost fields b, c ensure that the correct measure is obtained.

The light-cone form of any field theoretic propagator, whether it is for a scalar, fermion, or gauge field is always simply the scalar propagator times a Kronecker delta that describes the flow of spin and other internal quantum numbers. Thus the expression (1) is a universal part of the worldsheet construction for any field. When internal degrees of freedom are also present, however, one must also give a local worldsheet description of them. In the case of pure Yang-Mills, this was accomplished by introducing a transverse vector valued Grassmann odd worldsheet field $S^k(\sigma, \tau)$ [6]. The absence of bulk dynamical variables on the worldsheet is evident from the absence of $\dot{\mathbf{q}}$ dependence in the action. This means that the bulk fields are determined

[¶]The light-cone components of a Minkowski vector v^μ are defined as $v^\pm = (v^0 \pm v^{D-1})/\sqrt{2}$, with the remaining (transverse) components of v^μ distinguished by Latin indices, or as a vector by bold-face type. The Lorentz invariant scalar product of two four vectors v, w is written $v \cdot w = \mathbf{v} \cdot \mathbf{w} - v^+w^- - v^-w^+$.

by their boundary values, which is the sense in which we describe the worldsheet system as topological. However boundary dynamics is implicit in the Dirichlet boundary conditions which correlate different time slices.

Note that a factor of $1/2p^+$ present in the usual bosonic propagator has been removed: it must therefore be included in the definition of the vertices. By convention we introduce m , a unit of p^+ , and include the dimensionless factor m/p^+ in the *earlier* of the two vertices connected by the propagator, and a factor $1/\sqrt{2m}$ in *each* of the two vertices. A cubic vertex is represented on the rectangular worldsheet just described by the appearance (or disappearance) at some time of an interior Dirichlet boundary at fixed σ . The value of \mathbf{q} on this boundary governs how the transverse momentum is shared among the particles. For example, a fission vertex is the appearance of a solid line, say at $\sigma = p_1^+$, representing the new boundary. Before this occurs the system is a single particle with momentum $\mathbf{p} = \mathbf{q}(p^+) - \mathbf{q}(0)$. Afterwards the system is two particles with momenta $\mathbf{p}_1 = \mathbf{q}(p_1^+) - \mathbf{q}(0)$, $\mathbf{p}_2 = \mathbf{q}(p^+) - \mathbf{q}(p_1^+)$. If the new boundary line subsequently terminates, the diagram contains an extra loop. Thus the sum over all planar diagrams in a theory with only cubic vertices is just the sum over all ways of inserting such boundary lines within the worldsheet. This sum can be accomplished technically by discretizing $\sigma = lm$ and $\tau = ka$ as in [5] and introducing an Ising spin variable on each temporal bond that keeps track of whether it is part of an interior boundary (drawn as a solid line) or not (drawn as a dotted line). The technical details of this procedure are described in [1, 6].

Quartic and higher point vertices would seem to spoil this nice worldsheet picture by introducing nonlocal features into the worldsheet description. It is therefore very satisfying that the quartic interactions required in Yang-Mills theory are automatically generated by the worldsheet formalism from the presence of two cubic vertices, which are linear in the transverse momenta [6]. Note that this does *not* happen in purely scalar field theory where quartic vertices would require a nonlocal worldsheet dynamics. The status of the worldsheet description of fermion fields also needs to be evaluated. Since supersymmetry requires the presence of fermion fields and extended supersymmetry the presence of additional scalar fields, we face the important question: which supersymmetric theories can be given a local worldsheet description? This article is devoted to answering this question.

A concise and very convenient way to specify the field content and couplings of a gauge theory with extended supersymmetry, is to begin with a $\mathcal{N} = 1$ gauge theory in higher dimensions $D > 4$ and then apply dimensional reduction. This means that all the fields are required to be independent of the $D - 4$ extra coordinates. Then the extra components of the gauge field become scalar fields from the four dimensional point of view, and the higher dimensional representation of the Dirac matrices account for the multiplicity of spin 1/2 fields needed for the extended supersymmetry. In this way, the $\mathcal{N} = 2$ supersymmetric gauge theory descends from $\mathcal{N} = 1$ in $D = 6$ dimensions and the $\mathcal{N} = 4$ case descends from $\mathcal{N} = 1$ in $D = 10$ dimensions. Applying this method to the worldsheet construction, the first step is to promote the worldsheet field \mathbf{q} to a $D - 2$ component vector. One must at the same time supplement the ghost system with a new b, c pair for each pair of new dimensions. Once this is done dimensional reduction is simply the imposition of true Dirichlet boundary conditions on the extra components of \mathbf{q} : $q^k = 0$ on *all* worldsheet boundaries for $k = 3, \dots, D - 2$. In other words, in the language of string theory we restrict the fields to a three brane. Of course, in addition to the new components of \mathbf{q} , one must also add new components to the Grassmann spin variables that are monitoring the flow of internal degrees of freedom through the worldsheet.

One might at first think that the new components of \mathbf{q} are complete dummies contributing nothing new to the dynamics, leaving only the extra Grassmann variables to enrich the physics of the system. After all, by construction the bulk variables have no dynamical significance, and by setting the boundary values of these extra components to zero, it seems one has completely eliminated their dynamical relevance. However, this is not the case because the *fluctuations* of the \mathbf{q} variables are instrumental in generating the quartic vertices from pairs of cubic vertices. Since some of the new quartic interactions exchange the $O(D - 4)$ quantum numbers carried by the scalars, it is clear that a local worldsheet description will *require* that these extra components of \mathbf{q} be present.

We begin our work in the next section by using the light-cone Feynman rules for gauge fields in general dimension $D \geq 4$ to construct the worldsheet system that will reproduce all the planar diagrams in four dimensions containing the gauge particles and scalars and their cubic vertices necessary for $\mathcal{N} = 1, 2, 4$ gauge theories. In section 3 we do the same for the fermion fields and their cubic interactions with the gauge particles and scalars. In Section 4 we turn to the quartic vertices. We show that the basic mechanism

for their generation, discovered in [6], applies here as well. However, we also find an interesting limitation to its applicability. The coefficients of some of the generated quartics are dimension dependent, whereas the desired ones are not. One can arrange the correct values of these coefficients only if one dimensionally reduces to 4 or less space-time dimensions.

In Section 5, we present a system of Grassmann worldsheet fields that locally describes the flow of internal degrees of freedom through planar diagrams. We find that it is sufficient to introduce two sets of spinor-valued variables S^a, \bar{S}^b , where a, b are the spinor indices associated with the transverse rotation group $O(D-2)$. Vertex insertions involve either S^a (\bar{S}^b) for a fermion (anti-fermion) entering the vertex or the bilinear $S^b \gamma_{ba}^k \bar{S}^a$ for a scalar or gauge particle entering the vertex. Since the number of fermions entering the vertex is always even, the overall vertex insertion will be Grassmann even. Finally in section 6 we present one loop calculations in enough detail to learn how coupling constant renormalization works in the worldsheet language. We note several intriguing features. First it is recalled that the cancellation of entangled ultraviolet and infrared divergences familiar in light-cone calculations happens locally on the world-sheet. Once this cancellation has been taken into account, the remaining coupling renormalization also has an interesting local worldsheet interpretation. In particular, it is found that the cancellations typical of supersymmetry happen locally. Some further discussion and concluding remarks are given in Section 7.

2 Gauge Theory in D Dimensions Reduced to 4

As described in the introduction, we will be studying theories that can be obtained by dimensional reduction from an $\mathcal{N} = 1$ gauge theory in D dimensions. The Lagrangian for such a theory is just

$$\mathcal{L} = -\frac{1}{4} \text{Tr} F_{\mu\nu} F^{\mu\nu} + i \text{Tr} \psi^\dagger \alpha^\mu (\partial_\mu \psi - ig [A_\mu, \psi]) \quad (2)$$

$$F_{\mu\nu} \equiv \partial_\mu A_\nu - \partial_\nu A_\mu - ig [A_\mu, A_\nu], \quad (3)$$

where $\alpha^\mu \equiv \Gamma^0 \Gamma^\mu$ with Γ^μ the D dimensional Dirac gamma matrices. In this section we concentrate only on the bosonic fields. Fermions will be discussed in the next section.

We work in light-cone gauge $A_- = 0$. After eliminating A_+ using the Gauss' law constraint we arrive at the density of P^-

$$\begin{aligned} \mathcal{P}^- \equiv & \frac{1}{2} \text{Tr} \partial_i A_j \partial_i A_j - \frac{g^2}{2} \text{Tr} \left[\left(\frac{1}{\partial_-} [A_k, \partial_- A_k] \right)^2 + A_i A_j [A_i, A_j] \right] \\ & + ig \text{Tr} \partial_- A_k \left[A_j \overleftrightarrow{\frac{\partial}{\partial_-}} A_j - A_k \overleftrightarrow{\frac{\partial}{\partial_-}} A_i - A_i \overleftrightarrow{\frac{\partial}{\partial_-}} A_k \right], \end{aligned} \quad (4)$$

so that $H = P^- = \int d\mathbf{x} dx^- \mathcal{P}^-$. Here we have introduced the shorthand notation

$$X \overleftrightarrow{\frac{\partial}{\partial_-}} Y \equiv X \frac{\partial}{\partial_-} Y - \left(\frac{\partial}{\partial_-} X \right) Y. \quad (5)$$

We easily see that the free propagator is just the scalar propagator times δ_{ij} . To construct the worldsheet system the cubic interactions are all-important.

2.1 Cubic Yang-Mills Vertices in General Dimension

We first express the cubic term P_1^- of P^- in momentum modes:

$$A_k = \int \frac{d^{D-1} p}{(2\pi)^{(D-1)/2} \sqrt{2p^+}} (a_k(p) e^{ix \cdot p} + a_k^\dagger(p) e^{-ix \cdot p}), \quad (6)$$

where $d^{D-1}p = dp^+ d^{D-2}p\theta(p^+)$ and $x \cdot p = \mathbf{x} \cdot \mathbf{p} - x^- p^+$. Then we find

$$P_1^- = - \int \frac{dp_1 dp_2 dp_3}{\sqrt{|p_1^+ p_2^+ p_3^+|}} \left[\text{Tr } a_{n_2}^\dagger(-p_2) a_{n_1}^\dagger(-p_1) a_{n_3}(p_3) + \text{Tr } a_{n_3}^\dagger(-p_3) a_{n_2}(p_2) a_{n_1}(p_1) \right] \times V^{n_1 n_2 n_3} \delta(p_1 + p_2 + p_3), \quad (7)$$

where $V^{n_1 n_2 n_3}$ is given by^{||}

$$V^{n_1 n_2 n_3} = \frac{g}{8\pi^{3/2}} \left\{ \delta_{n_1 n_2} \left(p_3^+ \left[\frac{p_1}{p_1^+} - \frac{p_2}{p_2^+} \right]^{n_3} + p_2^+ \left[\frac{p_1}{p_1^+} - \frac{p_3}{p_3^+} \right]^{n_3} + p_1^+ \left[\frac{p_3}{p_3^+} - \frac{p_2}{p_2^+} \right]^{n_3} \right) \right. \\ \left. + \delta_{n_1 n_3} \left(p_2^+ \left[\frac{p_3}{p_3^+} - \frac{p_1}{p_1^+} \right]^{n_2} + p_3^+ \left[\frac{p_2}{p_2^+} - \frac{p_1}{p_1^+} \right]^{n_2} + p_1^+ \left[\frac{p_3}{p_3^+} - \frac{p_2}{p_2^+} \right]^{n_2} \right) \right. \\ \left. + \delta_{n_2 n_3} \left(p_1^+ \left[\frac{p_2}{p_2^+} - \frac{p_3}{p_3^+} \right]^{n_1} + p_3^+ \left[\frac{p_2}{p_2^+} - \frac{p_1}{p_1^+} \right]^{n_1} + p_2^+ \left[\frac{p_1}{p_1^+} - \frac{p_3}{p_3^+} \right]^{n_1} \right) \right\}. \quad (8)$$

In the expression (7) it is understood that the p^+ argument of a is always positive, so it is implied that the range of integration is $-p_1^+, -p_2^+ > 0$. For practical calculations remember that, when spatial (p^k, p^+) momentum conservation is taken into account, all of the momentum differences appearing in (8) are proportional to the single momentum

$$\mathbf{K} \equiv p_2^+ \mathbf{p}_1 - p_1^+ \mathbf{p}_2 = p_3^+ \mathbf{p}_2 - p_2^+ \mathbf{p}_3 = p_1^+ \mathbf{p}_3 - p_3^+ \mathbf{p}_1, \quad (9)$$

so we can obtain the dramatic simplification

$$V^{n_1 n_2 n_3} = \frac{g}{4\pi^{3/2}} \left(\delta_{n_1 n_2} \frac{K^{n_3}}{p_3^+} + \delta_{n_1 n_3} \frac{K^{n_2}}{p_2^+} + \delta_{n_2 n_3} \frac{K^{n_1}}{p_1^+} \right). \quad (10)$$

However in translating to the BT worldsheet formalism, it is important to choose in each term a version of K that allows cancellation of the $1/p_r^+$ factor. We shall stick with the original form (8) which makes these choices in a cyclically symmetric manner and does not exploit momentum conservation.

To present supersymmetric gauge theory for $\mathcal{N} > 1$, we will, in addition to fermions, need additional scalars. These are most simply obtained by dimensionally reducing from an $\mathcal{N} = 1$ SUSY gauge theory in higher dimensions. Let $n = 1, 2, \dots, D-2$ label the components of transverse space. Then dimensional reduction to 4 dimensions is achieved by setting $p_k^n = 0$ for $n = 3, 4, \dots, D-2$, giving $D-4$ scalars, $\phi_k = A^{2+k}$. This is, of course, done not only for external momenta but also internally for all loop momenta, only the first two components of which are integrated. When the cubic vertex involves some of these scalars, only the two scalar-vector vertex is non-vanishing. Taking the scalars to be particles 1, 2, so that $n_1, n_2 > 2$ and $n_3 = 1, 2$, we see that the scalar-scalar-vertex only gets contributions from the first line of Eq. (8).

Now we consider how to set up the worldsheet system corresponding to this dimensionally reduced gauge theory. Worldsheet fields $q^n(\sigma, \tau)$ will be introduced for all $D-2$ components. However, the boundary conditions will vary depending on n . For $n = 1, 2$ we impose the usual Dirichlet conditions so that $q^n(p^+) - q^n(0) = p^n$. On the other hand we shall require the components $n = 3, \dots, D-2$ to strictly vanish on all boundaries. This is the worldsheet version of dimensional reduction: the physics resides on a D3-brane in the q space. As usual there will also be $(D-2)/2$ pairs of ghosts b_a, c_a , to ensure the correct measure.

The worldsheet for a cubic vertex will contain one interior boundary that terminates within the diagram and extends either to early or late times (see Fig.1). As in [6] the momentum factors of the cubic vertex are produced by the insertion of $\partial q / \partial \sigma$ at suitable points in the vicinity of the end of the interior boundary. In practice we put the worldsheet on a grid [5] by discretizing $\tau = ka, \sigma = lm$ for $k, l = 1, 2, \dots, q(\sigma, \tau) \rightarrow q_l^k$. Since p^+ is now restricted to discrete values, the p^+ conserving delta function is replaced by $1/m$ times a

^{||}The factor $g/8\pi^{3/2}$ is appropriate for dimensional reduction to 4 dimensions. Before reduction it started as $g_D 2^{-3/2} (2\pi)^{-(D-1)/2}$. To carry out the reduction one first compactifies each extra dimension so that $p \rightarrow 2\pi n/L$ and then takes $L \rightarrow 0$, so only the mode $n = 0$ is kept. Then the measure and a 's in (7) together provide a factor $(2\pi/L)^{(D-4)/2}$, producing $g_D L^{-(D-4)/2} \pi^{-3/2}/8$. Recalling that the appropriate coupling in 4 dimensions as $L \rightarrow 0$ is $g \equiv g_D L^{-(D-4)/2}$, we arrive at the quoted result.

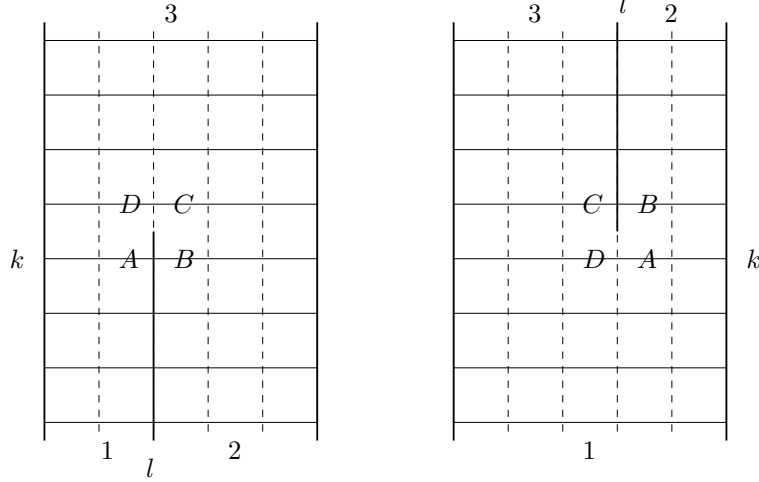


Figure 1: Discretized worldsheet for cubic fusion and fission vertices showing the possible locations of momentum insertions $\Delta\mathbf{q}$. We have labeled the four links surrounding the vertex A, B, C, D . For example an insertion at link A produces the factor \mathbf{p}_1/M_1 . Similarly, insertions at B, C produce the analogous factors for particles 2 and 3 respectively.

Kronecker delta. Further the vertex which is a matrix element of $-idx^+P_1^- \rightarrow -aP_1^-$. Thus the vertex function will be

$$\Gamma^{n_1 n_2 n_3} = \frac{a}{m} V^{n_1 n_2 n_3}, \quad (11)$$

where each $p_k^+ \equiv M_k m$ is now discrete. A single discretized insertion $\Delta\mathbf{q}_L = \mathbf{q}_{l+1}^k - \mathbf{q}_l^k$, where the link L is bounded by $l, l+1$, placed anywhere on the worldsheet of a single string has the expectation value \mathbf{p}/M . Note that since $p^k = 0$ for $k = 3, \dots, D-2$, the cubic vertex will be correctly produced whether the index k of q runs over just $k = 1, 2$ or over the whole set $k = 1, 2, \dots, D-2$. We shall require both choices, which we shall distinguish with a hat over the q if $k = 1, 2$ only, and no hat if it runs over just the whole range $k = 1, \dots, D-2$. The complete vertex insertion is then a sum over three kinds of terms, each with the insertion on a different string, *i.e.* on a different bond A, B , or C in Fig. 1. The factor multiplying each such insertion involves Kronecker delta's in the polarizations and is linear in the M_i , which we shall write in terms of those of the two particle state. Thus at a fusion vertex we write the total vertex function as

$$\begin{aligned} V_{fusion}^{n_1 n_2 n_3} \rightarrow \bar{V}^{n_1 n_2 n_3} &= \frac{g}{8\pi^{3/2}} (\delta_{n_1 n_2} [-M_1 \Delta q_A^{n_3} + M_2 \Delta q_B^{n_3} + (M_1 - M_2) \Delta \hat{q}_C^{n_3}] \\ &\quad + \delta_{n_1 n_3} [M_1 \Delta q_A^{n_2} - (2M_1 + M_2) \Delta \hat{q}_B^{n_2} + (M_1 + M_2) \Delta q_C^{n_2}] \\ &\quad + \delta_{n_2 n_3} [(2M_2 + M_1) \Delta \hat{q}_A^{n_1} - M_2 \Delta q_B^{n_1} - (M_1 + M_2) \Delta q_C^{n_1}]). \end{aligned} \quad (12)$$

On the other hand we write the insertion at a fission vertex as

$$\begin{aligned} V_{fission}^{n_1 n_2 n_3} \rightarrow V^{n_1 n_2 n_3} &= \frac{g}{8\pi^{3/2}} (\delta_{n_1 n_2} [(M_2 + M_3) \Delta q_A^{n_3} + M_2 \Delta q_B^{n_3} - (M_3 + 2M_2) \Delta \hat{q}_C^{n_3}] \\ &\quad + \delta_{n_1 n_3} [-(M_2 + M_3) \Delta q_A^{n_2} + (2M_3 + M_2) \Delta \hat{q}_B^{n_2} - M_3 \Delta q_C^{n_2}] \\ &\quad + \delta_{n_2 n_3} [(M_2 - M_3) \Delta \hat{q}_A^{n_1} - M_2 \Delta q_B^{n_1} + M_3 \Delta q_C^{n_1}]). \end{aligned} \quad (13)$$

Remember that in the fission case M_2 and M_3 are both negative. Note the occurrence of both hatted and unhatted q 's in these expressions: we shall see that this is essential in order for the fluctuations of q to produce the correct quartic vertices. The task of representing the remaining M_i dependence locally on the worldsheet will be handled in the next subsection.

2.2 Polynomials in p^+

As in [6] we handle the factors of M_i of Eqs (12), (13) by more ghost degrees of freedom, β, γ and $\bar{\beta}, \bar{\gamma}$. On each time slice we insert

$$\int \prod_{i=1}^{M-1} d\gamma_i d\beta_i d\bar{\gamma}_i d\bar{\beta}_i \exp \left\{ \beta_1 \gamma_1 + \sum_{i=1}^{M-2} (\beta_{i+1} - \beta_i)(\gamma_{i+1} - \gamma_i) + \bar{\beta}_{M-1} \bar{\gamma}_{M-1} + \sum_{i=1}^{M-2} (\bar{\beta}_{i+1} - \bar{\beta}_i)(\bar{\gamma}_{i+1} - \bar{\gamma}_i) \right\} = 1. \quad (14)$$

Here we have dispensed with the factors of 2π and a/m present in the b, c path integral. This insertion is completely harmless because it does nothing. But with these dummy-ghost systems available, we can locally produce factors of M_i at will as they are needed. For example, either $e^{\beta_{M-1}\gamma_{M-1}}$ applied on the right of a strip of M bits or $e^{\bar{\beta}_1\bar{\gamma}_1}$ applied on the left of the strip produces a factor of M . At a fusion vertex, the end of a solid line marks where two strips, 1 to the left of 2, join a single larger strip 3. Then an insertion of the first type on strip 1 produces M_1 , of the second type on strip 2 produces M_2 , and the sum of the two insertions produces $M_1 + M_2 = -M_3$. Similarly at a fission vertex a larger strip 1 joins two strips, 2 to the right of 3. Then an insertion of the first type on strip 3 produces $-M_3$, of the second type on strip 2 produces $-M_2$, and the sum of the two insertions produces $-M_2 - M_3 = M_1$. Thus we make the substitutions

$$\begin{aligned} M_1 &\rightarrow e^{\beta_A \gamma_A}, & M_2 &\rightarrow e^{\bar{\beta}_B \bar{\gamma}_B}, & \text{for fusion (Eq. 12),} \\ M_2 &\rightarrow -e^{\beta_B \gamma_B}, & M_3 &\rightarrow -e^{\bar{\beta}_C \bar{\gamma}_C}, & \text{for fission (Eq. 13).} \end{aligned} \quad (15)$$

All together we therefore have

$$\begin{aligned} \bar{V}^{n_1 n_2 n_3} &= \frac{g}{8\pi^{3/2}} \left(\delta_{n_1 n_2} \left[-e^{\beta_A \gamma_A} \Delta q_A^{n_3} + e^{\bar{\beta}_B \bar{\gamma}_B} \Delta q_B^{n_3} + (e^{\beta_A \gamma_A} - e^{\bar{\beta}_B \bar{\gamma}_B}) \Delta \hat{q}_C^{n_3} \right] \right. \\ &\quad + \delta_{n_1 n_3} \left[e^{\beta_A \gamma_A} \Delta q_A^{n_2} - (2e^{\beta_A \gamma_A} + e^{\bar{\beta}_B \bar{\gamma}_B}) \Delta \hat{q}_B^{n_2} + (e^{\beta_A \gamma_A} + e^{\bar{\beta}_B \bar{\gamma}_B}) \Delta q_C^{n_2} \right] \\ &\quad \left. + \delta_{n_2 n_3} \left[(2e^{\bar{\beta}_B \bar{\gamma}_B} + e^{\beta_A \gamma_A}) \Delta \hat{q}_A^{n_1} - e^{\bar{\beta}_B \bar{\gamma}_B} \Delta q_B^{n_1} - (e^{\beta_A \gamma_A} + e^{\bar{\beta}_B \bar{\gamma}_B}) \Delta q_C^{n_1} \right] \right), \quad (16) \end{aligned}$$

$$\begin{aligned} V^{n_1 n_2 n_3} &= \frac{g}{8\pi^{3/2}} \left(\delta_{n_2 n_3} \left[(e^{\bar{\beta}_C \bar{\gamma}_C} - e^{\beta_B \gamma_B}) \Delta \hat{q}_A^{n_1} + e^{\beta_B \gamma_B} \Delta q_B^{n_1} - e^{\bar{\beta}_C \bar{\gamma}_C} \Delta q_C^{n_1} \right] \right. \\ &\quad + \delta_{n_1 n_3} \left[(e^{\beta_B \gamma_B} + e^{\bar{\beta}_C \bar{\gamma}_C}) \Delta q_A^{n_2} - (2e^{\bar{\beta}_C \bar{\gamma}_C} + e^{\beta_B \gamma_B}) \Delta \hat{q}_B^{n_2} + e^{\bar{\beta}_C \bar{\gamma}_C} \Delta q_C^{n_2} \right] \\ &\quad \left. + \delta_{n_1 n_2} \left[(e^{\bar{\beta}_C \bar{\gamma}_C} + 2e^{\beta_B \gamma_B}) \Delta \hat{q}_C^{n_3} - (e^{\beta_B \gamma_B} + e^{\bar{\beta}_C \bar{\gamma}_C}) \Delta q_A^{n_3} - e^{\beta_B \gamma_B} \Delta q_B^{n_3} \right] \right). \quad (17) \end{aligned}$$

2.3 Quartic Vertices

We quote here the expressions for the complete quartic vertices, combining those from ‘‘Coulomb’’ exchange with those from the $\text{Tr}[A_i, A_j]^2$ term in the Lagrangian, manipulated into a form that suggests a concatenation of two cubics. In Cartesian basis we can write them in the following way:

$$\begin{aligned} \Gamma^{i_1 i_2 i_3 i_4} &= \frac{g^2 a}{32m\pi^3} \left\{ \delta_{i_1 i_2} \delta_{i_3 i_4} \frac{(p_1^+ - p_2^+)(p_4^+ - p_3^+)}{(p_1^+ + p_2^+)^2} + (\delta_{i_1 i_3} \delta_{i_2 i_4} - \delta_{i_1 i_4} \delta_{i_2 i_3}) \right\} \\ &\quad + \frac{g^2 a}{32m\pi^3} \left\{ \delta_{i_2 i_3} \delta_{i_1 i_4} \frac{(p_1^+ - p_4^+)(p_2^+ - p_3^+)}{(p_1^+ + p_4^+)^2} + (\delta_{i_1 i_3} \delta_{i_2 i_4} - \delta_{i_1 i_2} \delta_{i_3 i_4}) \right\}, \quad (18) \end{aligned}$$

where as before all p_k^+ are taken to flow *into* the vertex, and the rearrangement factor $a/32m\pi^3$ has also been included. The first line on the right side looks like the exchange of an $O(D-2)$ singlet and an $O(D-2)$ antisymmetric tensor in the s channel (12,34) and the second line like the same exchanges in the t channel (23,41). We shall discuss how these quartic vertices as well as quartics that involve fermion legs are produced from pairs of cubics in Section 4.

3 Fermion Fields

In this section, we will extend our discussion to the fermion case and thus to the supersymmetric theories. In particular, we are interested in the $\mathcal{N} = 1, 2$ and $\mathcal{N} = 4$ supersymmetric gauge theories.

We begin with the fermion part of the Lagrangian (3)

$$\mathcal{L}_{Dirac} = i\text{Tr} [\psi^\dagger \Gamma^0 \Gamma^\mu (\partial_\mu \psi - ig[A_\mu, \psi])], \quad (19)$$

and the Dirac equation is

$$\Gamma^\mu (\partial_\mu \psi - ig[A_\mu, \psi]) = 0. \quad (20)$$

On the lightcone one eliminates half of the components of ψ by writing $\psi = \psi^+ + \psi^-$, with $\psi^\pm \equiv \Gamma^\pm \Gamma^\mp \psi / 2$, so $\Gamma^\pm \psi^\pm = 0$. Then the equation for ψ^+ doesn't involve time derivatives, and so these components can be explicitly eliminated:

$$\psi^+ = -\frac{1}{2\partial_-} \Gamma^+ \Gamma^k (\partial_k \psi^- - ig[A_k, \psi^-]). \quad (21)$$

In the notation introduced in the appendix, ψ^+ consists of the checked components $\psi^{\check{a}}$ and ψ^- the unchecked components ψ^b , where the indices \check{a}, b each run over $2^{(D-2)/2}$ values. Thus we may also express this relation as

$$\psi^{\check{a}} = -\frac{1}{\sqrt{2}\partial_-} (\Gamma^0 \Gamma^k)_{\check{a}b} (\partial_k \psi^b - ig[A_k, \psi^b]). \quad (22)$$

In the light-cone gauge, after eliminating A_+ and $\psi^{\check{a}}$ using Eq. (22), we obtain the Lagrangian density

$$\begin{aligned} \mathcal{L} = & i\text{Tr} \left[\psi^{b\dagger} \left(\partial_+ - \frac{\nabla^2}{2\partial_-} \right) \psi^b \right] + \frac{g^2}{2} \text{Tr} \left(\{ \psi^a, \psi^{a\dagger} \} \frac{1}{\partial_-^2} \{ \psi^b, \psi^{b\dagger} \} \right) \\ & - i g^2 \text{Tr} \left(\frac{1}{\partial_-^2} [\partial_- A_k, A_k] \{ \psi^b, \psi^{b\dagger} \} \right) - \frac{g}{2} \text{Tr} \left\{ \frac{\partial_n}{\partial_-} \psi^{c\dagger} (\delta^{nk} + i \Sigma^{nk})_{cb} [A_k, \psi^b] \right\} \\ & - \frac{g}{2} \text{Tr} \left\{ [\psi^{c\dagger}, A_n] (\delta^{nk} + i \Sigma^{nk})_{cb} \frac{\partial_k}{\partial_-} \psi^b \right\} + g \text{Tr} \left(\psi^{b\dagger} \left[\frac{1}{\partial_-} \nabla \cdot A, \psi^b \right] \right) \\ & + \frac{ig^2}{2} \text{Tr} \left\{ [\psi^{c\dagger}, A_n] (\delta^{nk} + i \Sigma^{nk})_{cb} \frac{1}{\partial_-} [A_k, \psi^b] \right\}, \end{aligned} \quad (23)$$

where we rescaled $\psi \rightarrow 2^{-1/4} \psi$ in Eq. (23) and used the identity $\gamma^n \gamma^k = \delta^{nk} + i \Sigma^{nk}$.

As before, we expand the free fermion field in momentum modes

$$\psi^a(x) = \int \frac{d^{D-1}p}{(2\pi)^{(D-1)/2}} (b_a(p) e^{ix \cdot p} + d_a^\dagger(p) e^{-ix \cdot p}), \quad (24)$$

where we recall that $d^{D-1}p = dp^+ d^{D-2}p \theta(p^+)$ and $x \cdot p = \mathbf{x} \cdot \mathbf{p} - x^- p^+$.

From Eq. (23), one can see that the fermion free propagator in the mixed x^+, p^+, \mathbf{p} representation does not contribute factors of $1/p^+$ to the vertices, in contrast to the boson propagators. The lightcone mixed representation propagators with $p^+ > 0$ for the particles created by b^\dagger and d^\dagger are

$$\theta(x^+ - y^+) e^{-i(x^+ - y^+) \mathbf{p}^2 / 2p^+}, \quad -\theta(y^+ - x^+) e^{-i(y^+ - x^+) \mathbf{p}^2 / 2p^+}, \quad (25)$$

respectively. To construct a worldsheet system involving fermions, the cubic interactions are again the key ingredients. To extract the Feynman rule for a term in the Lagrangian, we first normal order the term and then assign the operators from left to right to the legs of the Feynman diagram going clockwise starting from

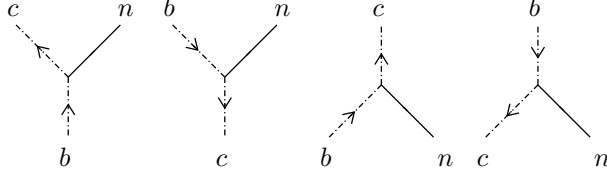


Figure 2: Fermion scattering vertices with gluon emitted or absorbed on the right.

the top left corner. This convention of reading off the Feynman rules for generic cubic and quartic terms in the Lagrangian can be summarized as follows:

$$\begin{array}{ccc}
 \text{Tr}(A^\dagger B^\dagger C) \rightarrow & \begin{array}{c} A \quad B \\ \diagdown \quad / \\ \quad \quad \quad | \\ \quad \quad \quad C \end{array} & \text{Tr}(A^\dagger BC) \rightarrow & \begin{array}{c} A \\ | \\ \diagup \quad \diagdown \\ C \quad B \end{array} & \text{Tr}(A^\dagger B^\dagger CD) \rightarrow & \begin{array}{c} A \quad B \\ \diagdown \quad / \\ \quad \quad \quad \diagup \quad \diagdown \\ C \quad D \end{array} & (26)
 \end{array}$$

3.1 Cubic fermion vertices in general dimensions

Following the analysis in section 2, we express the cubic term of Eq. (23) in momentum modes. The general structure of the cubic term is

$$\mathcal{L}_1 = \int \frac{dp_b dp_c dp}{\sqrt{p^+}} \text{Tr} [(FGF)_{cb}^k + (GFF)_{cb}^k + (FFG)_{cb}^k] V_{cb}^k \delta(p_b + p_c + p), \quad (27)$$

where G indicates any of the boson fields, F indicates the fermion field and

$$V_{cb}^n = \frac{g}{4\pi^{3/2}} \left[\frac{1}{2} (\gamma^n \gamma^k)_{cb} \left(\frac{p_b^k}{p_b^+} - \frac{p_c^k}{p_c^+} \right) + \delta_{cb} \left(\frac{p_c^n}{p_c^+} - \frac{p^n}{p^+} \right) \right]. \quad (28)$$

As noted in Section 2, the coupling constant in Eq. (28) is written in terms of the rescaled coupling constant appropriate to four-dimensions. Explicit forms of the above mentioned structures in Eq. (27) are

$$\begin{aligned}
 (FFG)_{cb}^k &= b_c^\dagger(-p_c) a_k(p) b_b(p_b) + b_c^\dagger(-p_c) a_k^\dagger(-p) b_b(p_b) \\
 &\quad + d_b^\dagger(-p_b) a_k(p) d_c(p_c) + d_b^\dagger(-p_b) a_k^\dagger(-p) d_c(p_c)
 \end{aligned} \quad (29)$$

$$\begin{aligned}
 (GFF)_{cb}^k &= a_k^\dagger(-p) b_c^\dagger(-p_c) b_b(p_b) + a_k^\dagger(-p) d_b^\dagger(-p_b) d_c(p_c) \\
 &\quad + d_b^\dagger(-p_b) d_c(p_c) a_k(p) + b_c^\dagger(-p_c) b_b(p_b) a_k(p)
 \end{aligned} \quad (30)$$

$$\begin{aligned}
 (FGF)_{cb}^k &= a_k^\dagger(-p) b_b(p_b) d_c(p_c) + a_k^\dagger(-p) d_c(p_c) b_b(p_b) \\
 &\quad + d_b^\dagger(-p_b) b_c^\dagger(-p_c) a_k(p) + b_c^\dagger(-p_c) d_b^\dagger(-p_b) a_k(p).
 \end{aligned} \quad (31)$$

Notice that from Eq. (25), there is a $(-)$ sign in the propagator for antiparticles, and there is also the overall $(-)$ included for each fermion loop. However in the worldsheet construction we would like to assign all net relative phases in diagrams to vertices, to achieve a local description. This can be done by modifying the above vertex assignments depending on which fermions are in initial and/or final states. The following scheme does the job. First, the vertices given above are taken for the case of particle scattering, when b is in the initial state and c is in the final state. For antiparticle scattering, when c is in the initial state and b in the final state, an extra minus sign is applied. The net effect of these two modifications is that particles and antiparticles are seen to couple to gluons in exactly the same way. Namely the vertices in Fig. 2, which correspond to Eq. (29), are assigned the factor $+V_{cb}^n$; and the vertices in Fig. 3, corresponding to Eq. (30), are assigned the factor $-V_{cb}^n$. For the annihilation and creation vertices, an extra minus sign is applied to the “counterclockwise” circulation of arrows. This means that all of these vertices, shown in

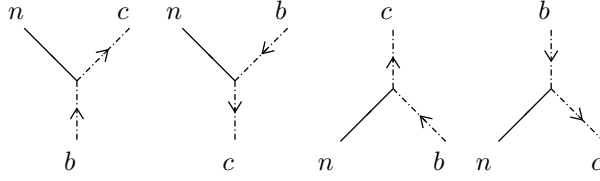


Figure 3: Fermion scattering vertices with gluon emitted or absorbed on the left.

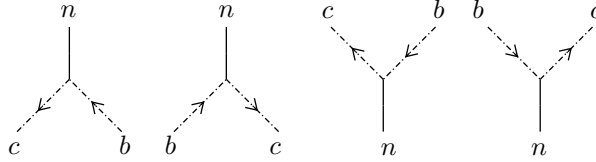


Figure 4: Fermion annihilation and creation vertices.

Fig. 4 and corresponding to Eq. (31) are assigned the factor $-V_{cb}^n$. With these modified vertex assignments all positive p^+ propagators are positive and there are no extra $-$ signs for fermion loops. This is the desired local assignment of phases arising from Fermi statistics.

Now we show how to set up the worldsheet system corresponding to this theory with interacting fermions and bosons (including both scalars and gluons). Using the notation of subsection 2.1, the cubic vertex factor is

$$V_{cb}^k = \frac{g}{4\pi^{3/2}} \left[\frac{1}{2} (\gamma^n \gamma^k)_{cb} (\Delta \hat{q}_b^k - \Delta \hat{q}_c^k) + \delta_{cb} \delta^{nk} (\Delta \hat{q}_c^k - \Delta \hat{q}^k) \right]. \quad (32)$$

Two points are worth comment. First of all, one can see from Eq. (32) that there is no factor of M_i , so one might have thought that one would not need to use the β, γ ghosts. However, as we shall see later in section 5 we do need β, γ ghosts to compensate factors which are produced by b, c ghost insertions, which are applied uniformly to all vertices. Secondly, the cubic vertex factor in Eq. (32) involves only $\Delta \hat{q}$. As we shall see later in section 4, this choice is necessary to produce the correct quartic vertices.

3.2 Fermion quartic vertices

We present here a complete list of fermion quartic vertices derived from (23). There are two groups of quartic vertices. One, which involves four fermions, is shown in Fig. 5 and the other, which has two fermion legs and two gluon legs, is depicted in Fig. 6, Fig. 7 and Fig. 8. among the four fermion quartic vertices, there are two types of quartic couplings: the first group is shown in Fig. 5-I) and 5-II), and the other is shown in Fig. 5-III) and 5-IV). Each of those shown in Fig. 5-I) and 5-II), has the coupling

$$-\frac{ag^2}{8m\pi^3} \left[\frac{1}{(p_a^+ + p_b^+)^2} \delta_{ab} \delta_{cd} - \frac{1}{(p_a^+ + p_d^+)^2} \delta_{ad} \delta_{bc} \right], \quad (33)$$

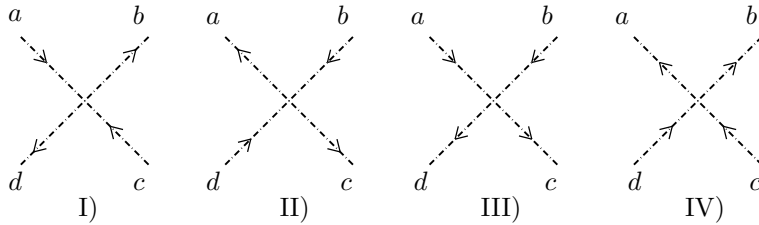


Figure 5: Four fermion quartic vertices.

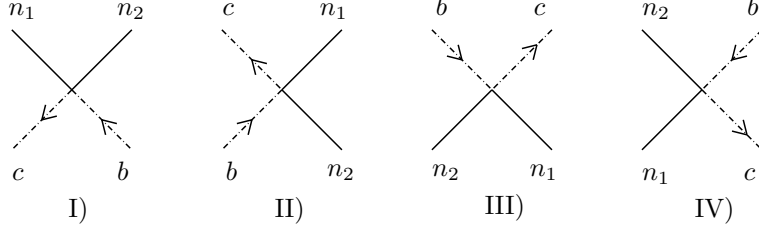


Figure 6: Two fermion and two gluon quartic vertices - 1.

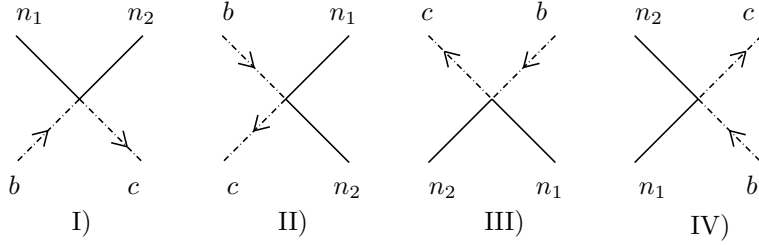


Figure 7: Two fermion and two gluon quartic vertices - 2.

whereas each shown in Fig. 5-III) and 5-IV) has the coupling

$$\frac{ag^2}{8m\pi^3} \frac{1}{(p_a^+ + p_d^+)^2} \delta_{ad} \delta_{bc} . \quad (34)$$

As one can see from the Lagrangian, there are several types of two fermion–two gluon quartic couplings. Each of the first type, shown in Fig. 6-I), Fig. 6-III) and Fig. 6-IV), has coupling

$$\frac{ag^2}{32m\pi^3} \left[2 \frac{p_1^+ - p_2^+}{(p_1^+ + p_2^+)^2} \delta^{n_1 n_2} \delta_{cb} + \frac{(\gamma^{n_1} \gamma^{n_2})_{cb}}{p_2^+ + p_b^+} \right], \quad (35)$$

whereas each shown in Fig. 6-II) have a coupling

$$-\frac{ag^2}{32m\pi^3} \left[2 \frac{p_1^+ - p_2^+}{(p_1^+ + p_2^+)^2} \delta^{n_1 n_2} \delta_{cb} + \frac{(\gamma^{n_1} \gamma^{n_2})_{cb}}{p_2^+ + p_b^+} \right]. \quad (36)$$

Another type of quartic vertices is shown in Fig. 7. In this case each of the vertices in Fig. 7-I), Fig. 7-III) and Fig. 7-IV) has the same coupling

$$\frac{ag^2}{32m\pi^3} \left[2 \frac{p_1^+ - p_2^+}{(p_1^+ + p_2^+)^2} \delta^{n_2 n_1} \delta_{cb} - \frac{(\gamma^{n_2} \gamma^{n_1})_{cb}}{p_1^+ + p_b^+} \right], \quad (37)$$

and Fig. 7-II) has the coupling

$$-\frac{ag^2}{32m\pi^3} \left[2 \frac{p_1^+ - p_2^+}{(p_1^+ + p_2^+)^2} \delta^{n_2 n_1} \delta_{cb} - \frac{(\gamma^{n_2} \gamma^{n_1})_{cb}}{p_1^+ + p_b^+} \right]. \quad (38)$$

The last type of two gluon-two fermion quartic vertices is depicted in Fig. 8. The coupling of Fig. 8-I) or Fig. 8-II) is

$$\frac{ag^2}{32m\pi^3} \left[\frac{(\gamma^{n_1} \gamma^{n_2})_{cb}}{p_2^+ + p_b^+} + \frac{(\gamma^{n_2} \gamma^{n_1})_{cb}}{p_1^+ + p_b^+} \right], \quad (39)$$

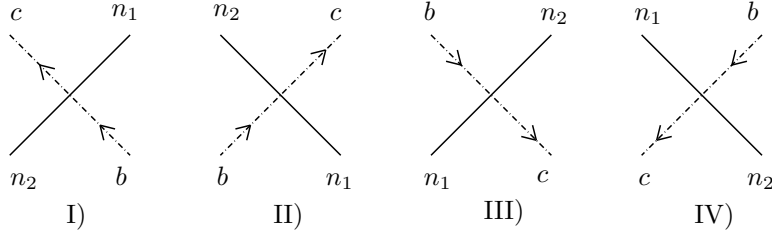


Figure 8: Two fermion and two gluon quartic vertices - 3.

while the coupling of Fig. 8-III) or Fig. 8-IV) is just

$$-\frac{ag^2}{32m\pi^3} \left[\frac{(\gamma^{n_1}\gamma^{n_2})_{cb}}{p_2^+ + p_b^+} + \frac{(\gamma^{n_2}\gamma^{n_1})_{cb}}{p_1^+ + p_b^+} \right]. \quad (40)$$

In Section 4, we shall discuss how these quartic vertices are correctly produced from pairs of boson and fermion cubic vertices.

4 Quartics from Cubics

In this section we show that the worldsheet mechanism for generating quartics from pairs of cubics identified in Ref. [6] applies also to the more general theories discussed here.

Recall from [6] that the scheme for spreading the propagator among M bits, involved the integral

$$I = \int d^2q_1 \cdots d^2q_{M-1} \exp \left\{ -\frac{a}{2m} \sum_{i=0}^{M-1} (\mathbf{q}_{i+1} - \mathbf{q}_i)^2 \right\} \equiv \int Dq e^{-S_q}. \quad (41)$$

and introduce the shorthand $\langle \cdots \rangle = \int Dq (\cdots) e^{-S_q} / I$. Then we recall from [6] the identities

$$\langle [\mathbf{q}_l - \mathbf{q}_{l-1}] \rangle = \frac{\mathbf{q}_M - \mathbf{q}_0}{M} \quad (42)$$

$$\left\langle (q_{i+1}^\alpha - q_i^\alpha)(q_{j+1}^\beta - q_j^\beta) \right\rangle = \left(\frac{q_M - q_0}{M} \right)^\alpha \left(\frac{q_M - q_0}{M} \right)^\beta + \frac{m}{a} \delta^{\alpha\beta} \delta_{ij} - \frac{m}{a} \frac{\delta^{\alpha\beta}}{M}. \quad (43)$$

The fluctuation terms of (43) cause two coincident cubics to behave as a quartic contact vertex. Because the $\Delta\mathbf{q}$ insertions on the three different worldsheet strips joined at a vertex are applied on two different time slices, we have the three possible fluctuation contributions shown in Fig. 9. The a) and b) contributions lead to the quartic vertices required by the Feynman rules. However, the c) contribution is eliminated by the double ghost insertion on one of the strips entering the vertex. In the next subsections, we shall discuss how to combine two cubic vertices into a quartic vertex.

4.1 Boson quartic vertex from two boson cubic vertices

In this subsection, we basically repeat arguments in Ref. [6] that a pair of cubic can combine to correctly produce a quartic vertex. However in the cases discussed here, in addition to gluons there are scalars as a consequence of dimensional reduction from higher dimensional theory. Therefore, we have here not only gluon exchange diagrams but also scalar exchange diagrams.

To see how a pair of two cubic vertices can correctly produce a quartic vertex, let us consider the four boson diagrams built from two cubics in Fig. 10. Using Eqs. (13) and (12), the product of two cubic vertex factors is

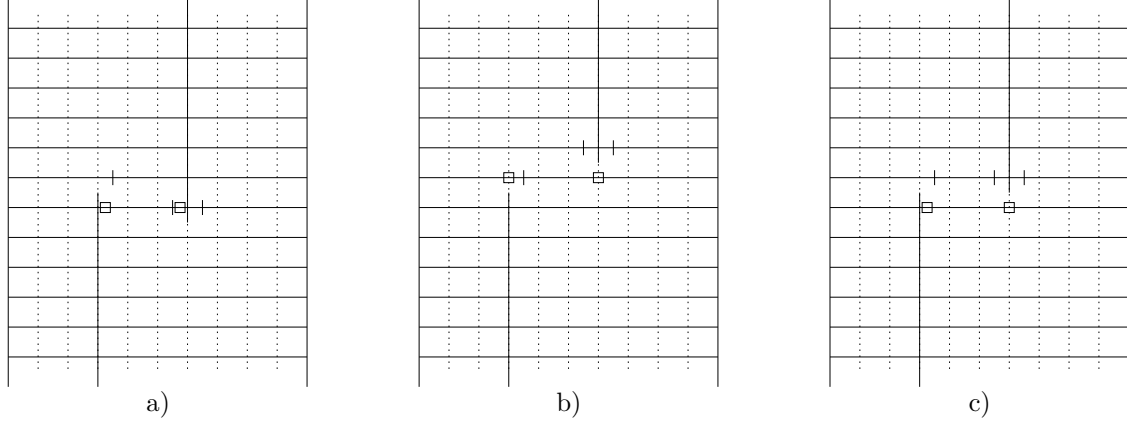


Figure 9: Possible contributions to the quantum term from two $\Delta \mathbf{q}$ insertions placed at the location of the open squares on the same time slice. Figures a) and b) produce the desired quartic vertices. The tick marks identify the ghost vertex insertions. The double insertion on strip 4 in figure c) provides a zero that suppresses this spurious quartic contribution.

$$\begin{aligned}
& \frac{g^2 a^2}{64m^2 \pi^3} [\delta_{n_1 n_2} \delta_{n_3 n_4} (M_1 - M_2)(M_3 - M_4) \Delta \hat{q}^{n_5} \Delta \hat{q}^{n_5} \\
& + \delta_{n_1 n_4} (M_1 + M_2)(M_3 + M_4) \Delta q^{n_2} \Delta q^{n_3} + \delta_{n_2 n_3} (M_1 + M_2)(M_3 + M_4) \Delta q^{n_1} \Delta q^{n_4} \\
& - \delta_{n_1 n_3} (M_1 + M_2)(M_3 + M_4) \Delta q^{n_2} \Delta q^{n_4} - \delta_{n_2 n_4} (M_1 + M_2)(M_3 + M_4) \Delta q^{n_1} \Delta q^{n_3}] \\
& + \frac{g^2 a^2}{64m^2 \pi^3} [\delta_{n_2 n_3} \delta_{n_1 n_4} (M_1 - M_4)(M_3 - M_2) \Delta \hat{q}^{n_5} \Delta \hat{q}^{n_5} \\
& + \delta_{n_1 n_2} (M_1 + M_4)(M_3 + M_2) \Delta q^{n_4} \Delta q^{n_3} + \delta_{n_4 n_3} (M_1 + M_4)(M_3 + M_2) \Delta q^{n_1} \Delta q^{n_2} \\
& - \delta_{n_1 n_3} (M_1 + M_4)(M_3 + M_2) \Delta q^{n_2} \Delta q^{n_4} - \delta_{n_2 n_4} (M_1 + M_4)(M_3 + M_2) \Delta q^{n_1} \Delta q^{n_3}]. \quad (44)
\end{aligned}$$

In this process fluctuation contributions of the type shown in Fig. 9a) and Fig. 9b) come from a double insertion on the intermediate string with momentum either $p_1 + p_2 = -p_3 - p_4$ or $p_1 + p_4 = -p_2 - p_3$. Remembering the $1/|M_1 + M_2|$ (or $1/|M_1 + M_4|$) factor from the intermediate propagator, the contribution of the quantum term is

$$\langle \Delta q^{n_1} \Delta q^{n_2} \rangle = -\frac{g^2 a}{32m\pi^3} \frac{\delta^{n_1 n_2}}{|M_1 + M_2|^2} \rightarrow \sum_n \langle \Delta q^n \Delta q^n \rangle = -\frac{g^2 a}{32m\pi^3} \frac{(D-2)}{|M_1 + M_2|^2}, \quad (45)$$

$$\langle \Delta \hat{q}^{n_5} \Delta \hat{q}^{n_5} \rangle = -\frac{g^2 a}{32m\pi^3} \frac{2}{|M_1 + M_2|^2}. \quad (46)$$

Note that the factor of 2 in Eq. (46) corresponds to the two transverse degrees of freedom of gluons (four dimensional gauge bosons). Eq. (45) yields precisely the contribution of the commutator squared term in the Yang-Mills Lagrangian (see Eq. (3)), while Eq. (46) produces the quartic vertex contribution from the induced instantaneous ‘‘Coulomb’’ exchange. Substituting Eqs. (45) and (46) into Eq. (44) and using momentum conservation in $D = 4$, it is not hard to show that the a) and b) type contributions correctly produce the quartic vertex in Eq. (18).

4.2 Fermion quartic vertices from two cubic vertices

Similarly to the previous subsection we shall show how two fermion cubic vertices also produce the quartic vertices. In principle, two cubic vertices should exchange either scalars, gluons or fermions to form quartic vertices. As we already saw in the boson case, to correctly produce the boson quartic vertex we needed both

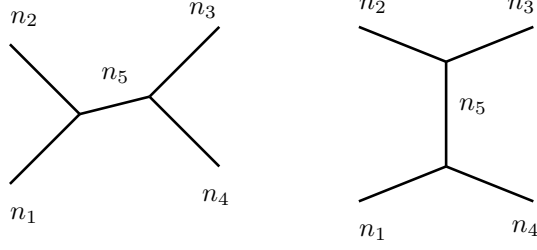


Figure 10: Gluon quartic vertex from two cubic vertices.

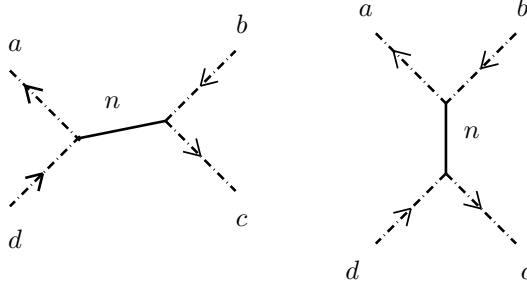


Figure 11: Four fermion quartic vertex from two cubic vertices exchange gluons.

gluon and scalar exchanges. In the fermion case, besides gluon exchange we also need fermion exchange but not scalar exchange. As before, the main fluctuation contributions are of the types shown in Fig. 9a) and Fig. 9b) while the unwanted contribution in Fig. 9c) due to zero propagation time for either gluon exchange or fermion exchange between two cubic vertices is eliminated using the b, c ghost insertion scheme. There are three distinct cases in which two cubic vertices form a quartic vertex. The first one, which involves gluon exchange, is shown in Fig. 11. Another process, which involves both gluon and fermion exchange, is depicted in Fig. 12. The last one shown in Fig. 13 involves only fermion exchange.

For the gluon exchange diagrams, there are two different contributions from s - and t -channels. The product of two cubic vertices of the first diagram (*i.e.* s -channel) in Fig. 11 is

$$\begin{aligned}
& -\frac{a^2 g^2}{16m^2 \pi^3} \times \left[\frac{1}{2} (\gamma^n \gamma^k)_{ad} (\Delta \hat{q}_d^k - \Delta \hat{q}_a^k) + \delta_{ad} \delta^{nk} (\Delta \hat{q}_a^k - \Delta \hat{q}_d^k) \right] \\
& \times \left[\frac{1}{2} (\gamma^n \gamma^l)_{cb} (\Delta \hat{q}_b^l - \Delta \hat{q}_c^l) + \delta_{cb} \delta^{nl} (\Delta \hat{q}_b^l - \Delta \hat{q}_c^l) \right]. \tag{47}
\end{aligned}$$

Notice that the only contribution in Eq. (47) comes from gluons. So one can write Eq. (47) as

$$-\frac{a^2 g^2}{16m^2 \pi^3} [\delta_{ad} \delta_{bc} \Delta \hat{q}^n \Delta \hat{q}^n], \tag{48}$$

and the quantum fluctuation term gives

$$\langle \Delta \hat{q}^n \Delta \hat{q}^n \rangle = -\frac{m}{a} \frac{2}{(p_a^+ + p_d^+)^2}. \tag{49}$$

So the contribution from s -channel gives us

$$\frac{a g^2}{8m \pi^3} \frac{\delta_{ad} d_{bc}}{(p_a^+ + p_d^+)^2}, \tag{50}$$

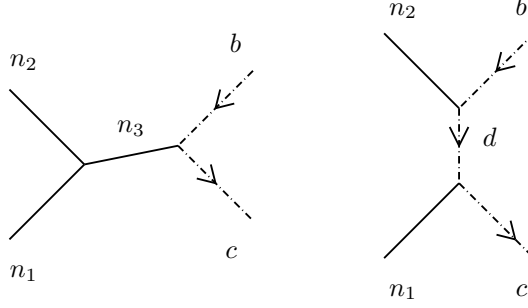


Figure 12: Quartic vertices involving fermions and gluons exchange both gluons and fermions.

where we already included the factor $1/|M_1 + M_4|$ from the gluon intermediate propagator. Similarly, one obtains for the t -channel

$$-\frac{ag^2}{8m\pi^3} \frac{\delta_{ab}d_{cd}}{(p_a^+ + p_b^+)^2}. \quad (51)$$

Combining Eqs. (50) and (51), it is easy to confirm that two cubic vertices indeed produce the four fermion quartic vertices shown in Fig. 5-II) with coupling (33). Notice that in this case only the instantaneous ‘‘Coulomb’’ exchanges contribute. Other diagrams of this type can be analyzed in the same way. Note that to produce diagrams Fig. 5-III) and 5-IV) one needs only the s -channel contribution.

For quartic vertices involving two fermions and two gluons, there are three different kinds of diagrams as shown in Figs. 6, 7 and 8. The first set of quartic vertices in Fig. 6 can be constructed from two cubic vertices which exchange both gluon and fermion as shown in Fig. 12. In this case the product of two cubic vertices from gluon exchange is

$$\begin{aligned} & -\frac{a^2g^2}{32m^2\pi^3} (\delta^{n_1n_2} [-(M_3 + M_2)\Delta q_A^{n_3} + (2M_2 + M_3)\Delta q_B^{n_3} - M_2\Delta \hat{q}_C^{n_3}] \\ & + \delta^{n_1n_3} [(M_3 + M_2)\Delta q_A^{n_2} + M_3\Delta \hat{q}_B^{n_2} - (M_2 + 2M_3)\Delta q_C^{n_2}] \\ & + \delta^{n_2n_3} [(M_3 - M_2)\Delta \hat{q}_A^{n_1} - M_3\Delta q_B^{n_1} + M_2\Delta q_C^{n_1}]) \\ & \times \left[\frac{1}{2}(\gamma^{n_3}\gamma^k)_{cb}(\Delta \hat{q}_b^k - \Delta \hat{q}_c^k) + \delta_{cb}\delta^{n_3k}(\Delta \hat{q}_c^k - \Delta \hat{q}^k) \right]. \end{aligned} \quad (52)$$

Because this is a gluon exchange diagram, the important terms are those hat momenta with upper index n_3 , *i.e.* Eq. (52) can be written as

$$+\frac{a^2g^2}{32m^2\pi^3}\delta^{n_1n_2}\delta_{cb}(M_3 + 2M_1)\Delta \hat{q}^{n_3}\Delta \hat{q}^{n_3} + \dots \quad (53)$$

Using our master formula (43) and $M_2 = -M_1 - M_3$, the above equation gives

$$\frac{ag^2}{16m\pi^2} \frac{p_1^+ - p_2^+}{(p_1^+ + p_2^+)^2} \delta^{n_1n_2}\delta_{cb}. \quad (54)$$

On the other hand, the product of two cubic vertices with fermion exchange shown in Fig. 12 is

$$\begin{aligned} & \frac{a^2g^2}{16m^2\pi^2} \left[\frac{1}{2}(\gamma^{n_1}\gamma^k)_{cd}(\Delta \hat{q}_d^k - \Delta \hat{q}_c^k) + \delta_{cd}(\Delta \hat{q}_c^{n_1} - \Delta \hat{q}^{n_1}) \right] \\ & \times \left[\frac{1}{2}(\gamma^l\gamma^{n_2})_{ab}(\Delta \hat{q}_d^l - \Delta \hat{q}_b^l) + \delta_{ab}(\Delta \hat{q}_b^{n_2} - \Delta \hat{q}^{n_2}) \right]. \end{aligned} \quad (55)$$

In this case the contribution comes from the hat momenta carrying spinor index d . Using our master formula (43) and momentum conservation $M_d = p_1^+ + p_c^+ = -(p_2^+ + p_b^+)$ (notice that $M_d > 0$) we obtain

$$\frac{ag^2}{32m\pi^3} \frac{(\gamma^{n_1}\gamma^{n_2})_{cb}}{p_2^+ + p_b^+}. \quad (56)$$

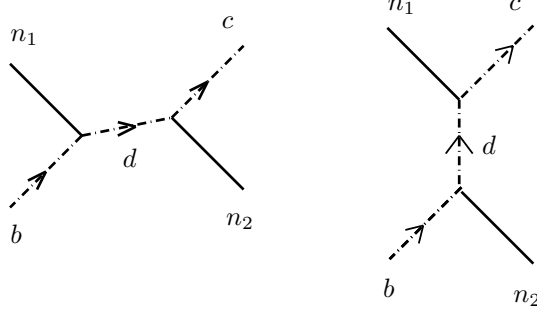


Figure 13: Quartic vertices involving fermions and gluons exchange fermions.

Combining Eqs. (54) and (56) one gets

$$\frac{ag^2}{32m\pi^2} \left[2 \frac{p_1^+ - p_2^+}{(p_1^+ + p_2^+)^2} \delta^{n_1 n_2} \delta_{cb} + \frac{(\gamma^{n_1} \gamma^{n_2})_{cb}}{p_2^+ + p_b^+} \right]. \quad (57)$$

The above equation is precisely a coupling of quartic vertex shown in Fig. 36-IV).

Similarly, we can show that the other set of quartic vertices involving two fermions and two gluons as depicted in Fig. 8 can be correctly reproduced by combining two cubic vertices. In this case there are two contributions coming from s - and t -channels of fermion exchange diagrams as shown Fig. 13. The product of two cubic vertices of this kind is

$$\begin{aligned} & -\frac{a^2 g^2}{16m^2 \pi^2} \left\{ \left[\frac{1}{2} (\gamma^{n_2} \gamma^k)_{db} (\Delta \hat{q}_b^k - \Delta \hat{q}_d^k) + \delta_{db} (\Delta \hat{q}_d^{n_2} - \Delta \hat{q}^{n_2}) \right] \times \right. \\ & \times \left[\frac{1}{2} (\gamma^{n_1} \gamma^l)_{cd} (\Delta \hat{q}_d^l - \Delta \hat{q}_c^l) + \delta_{cd} (\Delta \hat{q}_c^{n_1} - \Delta \hat{q}^{n_1}) \right] \\ & + \left[\frac{1}{2} (\gamma^{n_1} \gamma^k)_{db} (\Delta \hat{q}_b^k - \Delta \hat{q}_d^k) + \delta_{db} (\Delta \hat{q}_d^{n_1} - \Delta \hat{q}^{n_1}) \right] \times \\ & \left. \times \left[\frac{1}{2} (\gamma^{n_2} \gamma^l)_{cd} (\Delta \hat{q}_d^l - \Delta \hat{q}_c^l) + \delta_{cd} (\Delta \hat{q}_c^{n_2} - \Delta \hat{q}^{n_2}) \right] \right\}, \quad (58) \end{aligned}$$

where the first two lines are contributions from the t -channel while the last two are from the s -channel. Again using our master formula (43) we get

$$\frac{ag^2}{32m\pi^3} \left[\frac{(\gamma^{n_1} \gamma^{n_2})_{cb}}{p_2^+ + p_b^+} + \frac{(\gamma^{n_2} \gamma^{n_1})_{cb}}{p_1^+ + p_b^+} \right], \quad (59)$$

and the above equation is precisely the coupling which is shown in Fig. 8-II).

5 Grassmann Variables

In the case of pure Yang-Mills theory, the flow of vector polarization through a large planar diagram was described by Grassmann odd worldsheet spin variables \mathbf{S}_k , which carry transverse vector indices [6]. But since we must now deal with fermions as well, it is reasonable to instead attach spinor indices to the Grassmann variables. It will turn out that vector valued spin variables will not then be needed.

We first assume we have a complete Dirac multiplet of fermions, *i.e.* $2^{(D-2)/2}$ particles and the same number of anti-particles. In terms of the $O(D-2)$ Clifford algebra, the rotation generators for particles are $\Sigma^{kl}/2$ whereas those of the anti-particles are $-\Sigma^{kl*}/2$. (For a Majorana representation the two representations are identical.) Thus we introduce Grassmann variables S_k^a to describe the particle spin states and \bar{S}_k^a to describe the anti-particle spin states. Here a is an $O(D-2)$ spinor index and k labels the location of the

variable on the worldsheet, which will be specified in more detail later. Let us first consider a single chain $(S_1^a, \bar{S}_1^a), (S_2^a, \bar{S}_2^a), \dots, (S_{2K}^a, \bar{S}_{2K}^a)$, with an *even* number of spin variables, each carrying a spinor index and use the action

$$\mathcal{A} = \sum_{i=1}^{2K-1} \bar{S}_i^a S_{i+1}^a + \sum_{i=1}^{2K-1} S_i^a \bar{S}_{i+1}^a. \quad (60)$$

We define the measure for integration of the Grassmann variables by

$$\mathcal{D}S \equiv \prod_a [dS_{2K}^a dS_{2K-1}^a \cdots dS_1^a] [d\bar{S}_{2K}^a d\bar{S}_{2K-1}^a \cdots d\bar{S}_1^a]. \quad (61)$$

Then it is easy to check that

$$\langle e^{\bar{\eta}_1^a S_1^a + \eta_1^a \bar{S}_1^a + \bar{\eta}_{2K}^a S_{2K}^a + \eta_{2K}^a \bar{S}_{2K}^a} \rangle = e^{\bar{\eta}_{2K}^a \eta_1^a + \eta_{2K}^a \bar{\eta}_1^a}, \quad (62)$$

where $\langle \cdots \rangle \equiv \int \mathcal{D}S e^{\mathcal{A}}(\cdots)$. In particular, the last equation implies

$$\langle S_1^a \bar{S}_{2K}^b \rangle = \langle \bar{S}_1^a S_{2K}^b \rangle = \delta_{ab} \quad (63)$$

$$\langle \bar{S}_1^a \bar{S}_{2K}^b \rangle = \langle S_1^a S_{2K}^b \rangle = 0. \quad (64)$$

Note that these formulas *require* an even number of spins. In order to guarantee the consistent application of the even spin formal in the presence of interactions, the number of spins assigned to each bit must be a multiple of four. Eq. 64 will be used to supply the spinor Kronecker delta's for fermion propagators. To supply the Kronecker delta's for the vector and scalar particles, we could introduce vector valued spinors as in [6]. However, it will be more convenient to instead employ the bilinear $J^j \equiv 2^{-(D-2)/4} S_k^a \gamma_{ab}^j \bar{S}_k^b$. For this scheme to work, it is important that it produces the relations

$$\langle S_1^a J_{2K}^j \rangle = \langle \bar{S}_1^a J_{2K}^j \rangle = \langle J_1^j S_{2K}^a \rangle = \langle J_1^j \bar{S}_{2K}^a \rangle = 0 \quad (65)$$

$$\langle J_1^i J_{2K}^j \rangle = \delta_{ij}. \quad (66)$$

The first line is trivially true. The left side of the second equation is just $2^{-(D-2)/2} \gamma_{ab}^i \gamma_{ba}^j$, with repeated indices summed which is just $2^{-(D-2)/2} \text{Tr} \gamma^i \gamma^j = \delta_{ij}$, as desired.

The purpose of the Grassmann variables is to give a worldsheet local formalism to transport the spin and polarization information from the external lines to the point within the worldsheet where the interaction occurs. For the propagator we arrange the spin chain to visit every site on the lattice worldsheet, by snaking it through as shown in Fig. 14.

Next we turn to interactions. We draw the worldsheets for the fusion and fission cubic vertices in Fig. 15. The three open circles, on the bonds we have marked A , C , and D in Fig. 1, indicate the spins, which we label by the same letters, that participate in the vertex insertion that is designed to yield the correct cubic vertex. Let k label the time slice just before the solid line ends or begins and let l label the spatial location of the solid line. In constructing the vertex we need to refer to variables on the four spatial links immediately surrounding the vertex. For this purpose we use the A, B, C, D labeling scheme indicated in Fig. 1. We must also remember the ghost insertions that produce the factors of $1/|M_i|$ reassigned from the field theoretic bosonic propagator to the *earlier* vertex attached to it. Thus we insert $e^{-a\Delta b_C \Delta c_C/m}$ in the fusion vertex and $e^{-a(\Delta b_B \Delta c_B + \Delta b_C \Delta c_C)/m}$ in the fission vertex. We shall apply these same insertions to vertices involving fermion lines, even though the fermion propagator had no such factors of $1/|M_i|$ to begin with. This means that the vertices involving fermions will include additional factors of $|M_i|$ in the numerator to cancel the effects of the ghost insertions. The contribution of the 3 boson vertices to the insertion is simply a product of three bilinears J^k times one of the expressions (16) or (17). The contribution of the fermions requires a more elaborate notation because there are six distinct vertex types. We therefore define the following three bilocal bilinears:

$$\begin{aligned} \bar{J}_{DA}^j &= \frac{g}{8\pi^{3/2}} \{ S_D^c \bar{S}_A^b [(\gamma^j \gamma^k)_{cb} (\Delta \hat{q}_A^k - \Delta \hat{q}_C^k) + 2\delta_{cb} (\Delta \hat{q}_C^k - \Delta \hat{q}_B^k)] \\ &\quad + \bar{S}_D^b S_A^c [(\gamma^j \gamma^k)_{cb} (\Delta \hat{q}_C^k - \Delta \hat{q}_A^k) + 2\delta_{cb} (\Delta \hat{q}_A^k - \Delta \hat{q}_B^k)] \} (e^{\beta_A \gamma_A} + e^{\beta_B \bar{\gamma}_B}) \end{aligned} \quad (67)$$

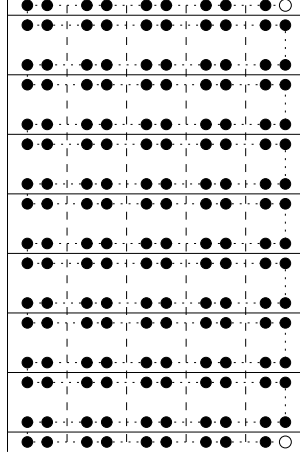


Figure 14: Assignment of Grassmann spins for propagator. Each dot is assigned Grassmann spins S_k^a, \bar{S}_k^a , and the bond pattern for the spin chain is indicated by dotted lines. External state information is specified by inserting S_k^a, \bar{S}_k^a or the bilinear J_k^j at the open circles.

$$\begin{aligned} \bar{\mathcal{J}}_{CD}^j &= \frac{g}{8\pi^{3/2}} \{ S_C^c \bar{S}_D^b [(\gamma^j \gamma^k)_{cb} (\Delta \hat{q}_B^k - \Delta \hat{q}_C^k) + 2\delta_{cb} (\Delta \hat{q}_C^k - \Delta \hat{q}_A^k)] \\ &\quad + \bar{S}_C^b S_D^c [(\gamma^j \gamma^k)_{cb} (\Delta \hat{q}_C^k - \Delta \hat{q}_B^k) + 2\delta_{cb} (\Delta \hat{q}_B^k - \Delta \hat{q}_A^k)] \} (e^{\beta_A \gamma_A} + e^{\bar{\beta}_B \bar{\gamma}_B}) \end{aligned} \quad (68)$$

$$\begin{aligned} \bar{\mathcal{J}}_{AC}^j &= \frac{g}{8\pi^{3/2}} \{ S_A^c \bar{S}_C^b [(\gamma^j \gamma^k)_{cb} (\Delta \hat{q}_B^k - \Delta \hat{q}_A^k) + 2\delta_{cb} (\Delta \hat{q}_A^k - \Delta \hat{q}_C^k)] \\ &\quad + \bar{S}_A^b S_C^c [(\gamma^j \gamma^k)_{cb} (\Delta \hat{q}_A^k - \Delta \hat{q}_B^k) + 2\delta_{cb} (\Delta \hat{q}_B^k - \Delta \hat{q}_C^k)] \}, \end{aligned} \quad (69)$$

for the fusion case, and a similar set for the fission case:

$$\begin{aligned} \mathcal{J}_{DA}^j &= \frac{g}{8\pi^{3/2}} \{ S_D^c \bar{S}_A^b [(\gamma^j \gamma^k)_{cb} (\Delta \hat{q}_A^k - \Delta \hat{q}_B^k) + 2\delta_{cb} (\Delta \hat{q}_B^k - \Delta \hat{q}_C^k)] \\ &\quad + \bar{S}_D^b S_A^c [(\gamma^j \gamma^k)_{cb} (\Delta \hat{q}_B^k - \Delta \hat{q}_A^k) + 2\delta_{cb} (\Delta \hat{q}_A^k - \Delta \hat{q}_C^k)] \} e^{\bar{\beta}_B \bar{\gamma}_B} \end{aligned} \quad (70)$$

$$\begin{aligned} \mathcal{J}_{CD}^j &= \frac{g}{8\pi^{3/2}} \{ S_C^c \bar{S}_D^b [(\gamma^j \gamma^k)_{cb} (\Delta \hat{q}_A^k - \Delta \hat{q}_C^k) + 2\delta_{cb} (\Delta \hat{q}_C^k - \Delta \hat{q}_B^k)] \\ &\quad + \bar{S}_C^b S_D^c [(\gamma^j \gamma^k)_{cb} (\Delta \hat{q}_C^k - \Delta \hat{q}_A^k) + 2\delta_{cb} (\Delta \hat{q}_A^k - \Delta \hat{q}_B^k)] \} e^{\beta_C \gamma_C} \end{aligned} \quad (71)$$

$$\begin{aligned} \mathcal{J}_{AC}^j &= \frac{g}{8\pi^{3/2}} \{ S_A^c \bar{S}_C^b [(\gamma^j \gamma^k)_{cb} (\Delta \hat{q}_C^k - \Delta \hat{q}_B^k) + 2\delta_{cb} (\Delta \hat{q}_B^k - \Delta \hat{q}_A^k)] \\ &\quad + \bar{S}_A^b S_C^c [(\gamma^j \gamma^k)_{cb} (\Delta \hat{q}_B^k - \Delta \hat{q}_C^k) + 2\delta_{cb} (\Delta \hat{q}_C^k - \Delta \hat{q}_A^k)] \} e^{\beta_C \gamma_C + \bar{\beta}_B \bar{\gamma}_B}. \end{aligned} \quad (72)$$

Then the fusion and fission vertex insertions on the worldsheet are

$$\frac{\bar{\mathcal{V}}_l^k}{2\pi} = \frac{a}{m} \{ \bar{\mathcal{J}}_{DA}^j J_C^j + \bar{\mathcal{J}}_{CD}^j J_A^j + \bar{\mathcal{J}}_{AC}^j J_D^j + J_A^{n_1} J_C^{n_2} J_D^{n_3} \bar{V}^{n_1 n_2 n_3} \} e^{-a \Delta b_C \Delta c_C / m} \quad (73)$$

$$\frac{\mathcal{V}_l^k}{2\pi} = \frac{a}{m} \{ \mathcal{J}_{DA}^j J_C^j + \mathcal{J}_{CD}^j J_A^j + \mathcal{J}_{AC}^j J_D^j + J_A^{n_1} J_C^{n_2} J_D^{n_3} V^{n_1 n_2 n_3} \} e^{-a(\Delta b_B \Delta c_B + \Delta b_C \Delta c_C) / m}. \quad (74)$$

We refer the reader to [6] for the details of how these vertex insertions enter the worldsheet path integral (see especially Eqs. (24) and (27) of that work).

We now consider briefly how the preceding discussion must be modified to realize various super symmetries. The number of fermionic states must be reduced from the complete Dirac multiplet so far assumed. For $\mathcal{N} = 1, 2$ we must reduce the number by a factor of 2 and for $\mathcal{N} = 4$ by a factor of 4. A factor of 2 is easily achieved by making a Weyl restriction on the fermion field. In the basis we have described in the appendix, this is achieved by restricting the $O(D-2)$ spinor indices on the insertions S^a, \bar{S}^a to the first (or last) $2^{(D-4)/2}$ components. To distinguish these two sets of indices, we shall denote the first $2^{(D-4)/2}$

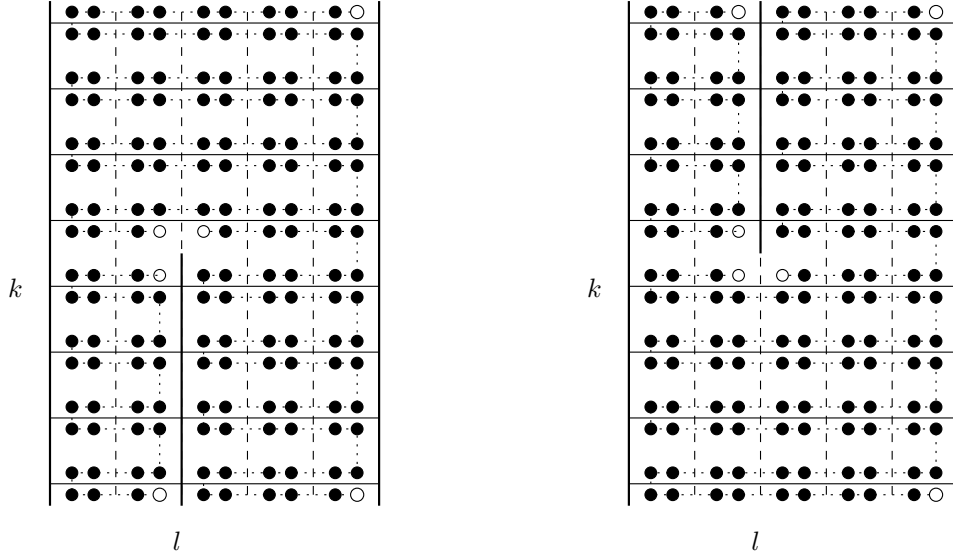


Figure 15: Cubic fusion and fission vertices. The open circles surrounding each interaction point are labeled by the same letters we have used to label the bonds they occur on in Fig. 1.

components by an undotted index a and put a dot over the index, \dot{a} if it labels the second $2^{(D-4)/2}$ components. Thus we start out with four distinct spinor types $S^a, S^{\dot{a}}, \bar{S}^a, \bar{S}^{\dot{a}}$, and the Weyl restriction means that we only insert S^a, \bar{S}^a on fermion lines. But the boson bilinears require the dotted indices as well $J^k = 2^{-(D-2)/2}(S^{\dot{a}}\gamma_{\dot{a}b}^k\bar{S}^b + S^a\gamma_{ab}^k\bar{S}^{\dot{b}})$, so the full complement of spinor indices is retained in the worldsheet path integral. This procedure takes care of the cases $\mathcal{N} = 1, 2$.

The $\mathcal{N} = 4$ case requires a further reduction of fermionic components by a factor of two. This is allowed because for $O(8)$ spinors can be made simultaneously Majorana and Weyl. In the Majorana representation, where γ^k are real (and symmetric) it is consistent to identify S and \bar{S} , so there is no distinction between particle and anti-particle. But then the bilinear $S^a\gamma_{ab}^k S^b + S^{\dot{a}}\gamma_{\dot{a}b}^k S^b$ is identically zero. However, precisely in this case we can redefine the bilinears as $J^k \equiv i2^{-(D-4)/2}S^a\gamma_{ab}^k S^b$. This modified definition works because we have

$$\langle J_1^k J_{2K}^l \rangle = -i^2 2^{-(D-4)/2} \gamma_{\dot{a}b}^k \gamma_{\dot{a}b}^l = 2^{-(D-4)/2} \text{Tr} \gamma^k \gamma^l \frac{1 + \gamma_9}{2} = \delta_{kl}. \quad (75)$$

Finally, we remark that the spinor-valued Grassmann odd variables we have introduced here can also be employed in the worldsheet for pure Yang-Mills theory instead of the vector-valued ones used in [6]. One simply restricts the insertions to *only* the bilinears J^k . We might then dub this case $\mathcal{N} = 0$ supersymmetry, and the formalism developed here then covers in a unified manner all the interesting 4 dimensional quantum field theories with $\mathcal{N} = 0, 1, 2, 4$ supersymmetry.

6 One Loop Renormalization

When using the discretized worldsheet to calculate processes to a given order in perturbation theory, we recall that the insertions have been designed to exactly reproduce the cubic vertices of the light-cone Feynman rules in the continuum limit. The precise meaning of this limit is that every solid line in the diagram is many lattice steps long and also is many lattice steps away from every other solid line. Clearly a diagram in which one of these criteria is not met is sensitive to the details of our discretization choice. In tree diagrams one can always avoid these dangerous situations by restricting the external legs so that they carry p_i^+ so that all differences $|p_i^+ - p_j^+| \gg m$, and so that the time of evolution between initial and final states $\tau \gg a$. However, a diagram containing one or more loops will involve sums over intermediate states that violate these inequalities, and because of field theoretic divergences the dangerous regions of these sums can

produce significant effects in the continuum limit. In particular we should expect these effects to include a violation of Lorentz invariance, in addition to the usual harmless effects that are absorbed into renormalized couplings. Indeed, when a solid line is of order a few lattice steps in length, it produces a gap in the gluon energy spectrum that is forbidden by Lorentz invariance. This effect can be canceled by a counter-term that represents a local modification of the worldsheet action. We conjecture that all counter-terms needed for a consistent renormalization program can be implemented by local modifications of the worldsheet dynamics. In this section we confirm this conjecture to one loop order in perturbation theory.

6.1 Gluon Self Energy

The gluon self energy to one loop can be extracted from the lowest order correction to a gluon propagator represented by a single solid line segment on a worldsheet strip as in Fig. 16. For the theories considered in

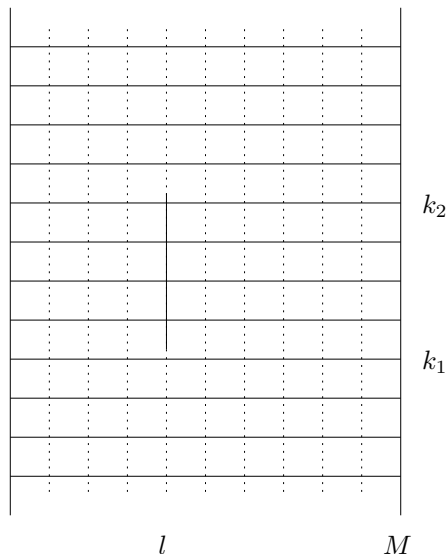


Figure 16: One loop self energy calculation. Because of time translation invariance only the difference $k = k_2 - k_1$ is important.

this article we must add the contribution of the fermions and scalars to the calculation in the pure Yang-Mills theory given in [15]. With our conventions the result analogous to Eqs. (52) and (53) of that article, for fixed k_1, k_2, l with $k = k_2 - k_1 > 1$ and $0 < l < M$, reads:

$$\Pi_{l,k} = \frac{g^2}{8\pi^2} \frac{u^k}{k^2} \left\{ \frac{2}{l} + \frac{2}{M-l} - \frac{1}{M} \left[4 - \frac{N_f}{2} - (2 + N_s - N_f) \frac{l}{M} \left(1 - \frac{l}{M} \right) \right] \right\}, \quad (76)$$

where $u = e^{-p^2 a/2Mm}$. This must be summed over l and k_1 and k_2 . For brevity in the discussion of these sums, denote by $A(l, M)$ the contents of the curly braces in the last equation. Now consider the one loop correction to the gluon propagator, propagating $K = T/a$ time steps. The loop starts at time $k_1 a$ and ends at $k_2 a$ and is positioned at $p^+ = ml$. Before introducing the counter-term we have the following expression for the propagator correction:

$$\begin{aligned} D_1(\mathbf{p}, M, K) &= \sum_{k_1=1}^{K-3} \sum_{k_2=k_1+2}^{K-1} u^{k_1} u^{K-k_2} \frac{g^2}{8\pi^2} \frac{u^{k_2-k_1}}{(k_2-k_1)^2} \sum_{l=1}^{M-1} A(l, M) \\ &= \frac{g^2}{8\pi^2} \sum_{k_1=1}^{K-3} \sum_{k_2=k_1+2}^{K-1} u^K \frac{1}{(k_2-k_1)^2} \sum_{l=1}^{M-1} A(l, M) \end{aligned}$$

$$= u^K \frac{g^2}{8\pi^2} \left[\left(\frac{\pi^2}{6} - 1 \right) K - \ln K + \mathcal{O}(K^0) \right] \sum_{l=1}^{M-1} A(l, M). \quad (77)$$

The term linear in K comes from terms where the loop is short ($k_2 - k_1 \ll K$) and the sum is over the possible locations of it. It is clear that when n short loops are summed over their locations we get factors proportional to $C^n K^n / n!$ where C is the coefficient of K in the above linear term. The short loop behavior therefore exponentiates and causes a shift of the “energy”, $a\mathbf{p}^2/2Mm$, in the exponent of the free propagator. This shift causes a gap in the gluon energy spectrum that is forbidden in perturbation theory by Lorentz invariance. We must therefore attempt to cancel this linear term in K order by order in perturbation theory with a suitable choice of counter-term. One simple choice is a two time step short loop of exactly the structure that went into the “bare” self-energy. Then at one loop order it will be proportional to the $k = 2$ term and will have the form:

$$e^{-ka\mathbf{p}^2/2mM} \frac{g^2}{4\pi^2} \frac{\xi k}{4} \sum_{l=1}^{M-1} A(l, M), \quad (78)$$

where we adjust ξ to cancel the term proportional to k in the propagator correction. Choosing $\xi = 4(1 - \pi^2/6)$ does the job and we are left with a logarithmic divergence which will be absorbed in the wave function contribution to coupling renormalization. We have: $\ln k = \ln(1/a) + \ln(T)$, with $T = ka$, the total evolution time. We can therefore absorb the divergence in the wave function renormalization factor:

$$Z(M) = 1 - \frac{g^2}{8\pi^2} \ln(1/a) \sum_{l=1}^{M-1} \left\{ \frac{2}{l} + \frac{2}{M-l} + \frac{F(l/M)}{M} \right\}, \quad (79)$$

where

$$F(x) = 2f_g(x) + N_f f_f(x) + N_s f_s(x) \quad (80)$$

$$f_i(x) = \begin{cases} x(1-x) - 2 & \text{for } i = g \text{ (gluons)} \\ x(1-x) & \text{for } i = s \text{ (scalars)} \\ 1/2 - x(1-x) & \text{for } i = f \text{ (fermions)}. \end{cases} \quad (81)$$

The first two terms in the l sum produce a $\ln(1/m)$ divergence and we notice the familiar entanglement of ultraviolet ($a \rightarrow 0$) and infrared ($m \rightarrow 0$) divergences [16]. It was explained how these divergences disentangle in [17] and we will discuss this further in subsection 6.3. In (80) N_f counts the total number of fermionic states, so, for example, a single Dirac fermion in 4 space-time dimensions has $N_f = 4$. We see that supersymmetry, $N_f = N_b = 2 + N_s$, kills the l dependent term in the summand. If $N_f = 8$ as well, the wave function contribution to coupling renormalization (apart from the entangled divergences) vanishes. This is the particle content of $\mathcal{N} = 4$ SUSY Yang-Mills theory.

6.2 Correction to Cubic Vertex with External Gluons

Now we turn to the contribution of the proper vertex to coupling renormalization. The proper one loop correction to the cubic vertex is represented by a Feynman triangle graph appearing in the worldsheet as shown in Fig. 17, which establishes our kinematics. With the external particles of Fig. 17 restricted to be gluons (vector bosons) the one loop renormalization of the gauge coupling requires calculating the triangle graph for the different particles of the theory running around the loop. In the following subsections it will be useful to employ the “complex basis” $x^\wedge = x^1 + ix^2$ and $x^\vee = x^1 - ix^2$ for the first two components of any transverse vector \mathbf{x} .

Fermions

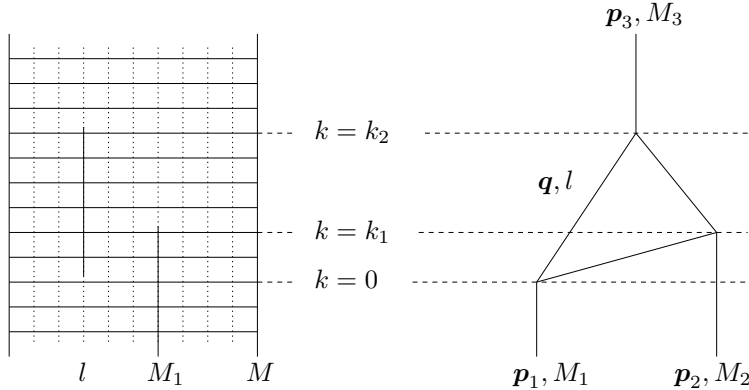


Figure 17: Basic kinematic setup for the one loop correction to the cubic vertex. The momenta p_1 and p_2 are taken to point into the vertex whereas p points out, so that momentum conservation reads $p_1 + p_2 \equiv p = -p_3$. In particular, $M \equiv M_1 + M_2 = -M_3$ is positive. We take the external gluon lines to have polarizations n_1, n_2, n_3 .

Referring to Appendix B for details of the calculation the result for the diagram depicted in Fig. 17 with fermions on the internal lines is given by:

$$(\Gamma_1^{\text{fermions}})^{\wedge\wedge\vee} = -\frac{N_f g^3}{4\pi^2} \frac{a}{m} \ln(1/a) \frac{p^+ K^\wedge}{p_1^+ p_2^+} \sum_{l=1}^{M_1-1} \frac{f_f(l/M)}{M} - (1 \leftrightarrow 2), \quad (82)$$

for polarizations $n_1 = n_2 = \wedge, n_3 = \vee$. We shall quote the result for other polarizations later. Recall that \mathbf{K} has been defined in Eqn. 9. Also the term $(1 \leftrightarrow 2)$ comes from the other time ordering $k_1 < 0$.

Gluons

This calculation has been done for $n_1 = n_2 = \wedge, n_3 = \vee$ in [17] and it is very similar to the fermion calculation. The contribution to charge renormalization is given by:

$$(\Gamma_1^{\text{gluons}})^{\wedge\wedge\vee} = -\frac{g^3}{4\pi^2} \frac{a}{m} \ln(1/a) \frac{p^+ K^\wedge}{p_1^+ p_2^+} \sum_{l=1}^{M_1-1} \left\{ \frac{2}{l} + \frac{1}{M-l} + \frac{1}{M_1-l} + \frac{2f_g(l/M)}{M} \right\} - (1 \leftrightarrow 2). \quad (83)$$

The first three logarithmically divergent terms in the l summands again represent the entanglement of infrared and ultraviolet divergences and we will see in section 6.3 how they cancel against similar terms from the self energy contribution.

Scalars

Now consider scalars on internal lines and the same external polarizations as before. Recall that the indices n_i in Eq. (8) run from 1 to $D-2$. Let us use indices a, b for directions 3 to $D-2$. Then dimensional reduction is implemented by taking $p_i^a = 0$ for all i and a . Using these conventions we will be interested in the special case of Eq. (8) with $n_1 = a, n_2 = b$ and $n_3 = \vee$:

$$\Gamma_0^{ab\vee} = \frac{g}{8\pi^{3/2}} \frac{a}{m} \delta^{ab} \frac{2K^\vee}{p_1^+ + p_2^+}, \quad (84)$$

and similarly for $\Gamma_0^{ab\wedge}$. The evaluation of the diagram is analogous to the previous calculations and the result

corresponding to (82) is:

$$(\Gamma_1^{\text{scalars}})^{\wedge\wedge\vee} = -\frac{N_s g^3}{4\pi^2} \frac{a}{m} \ln(1/a) \frac{p^+ K^\wedge}{p_1^+ p_2^+} \sum_{l=1}^{M_1-1} \frac{f_s(l/M)}{M} - (1 \leftrightarrow 2). \quad (85)$$

6.3 Discussion of results

The physical coupling can be measured by $\prod_i \sqrt{Z_i} \Gamma$, the renormalized vertex function, where Γ is the proper vertex and Z_i is the wave function renormalization for leg i . To one loop we write this in terms of our quantities as:

$$Y \equiv \Gamma_1 + \frac{1}{2} \Gamma_0 \sum_i (Z_i - 1), \quad (86)$$

where Γ_0 is the tree level vertex and Γ_1 is our one loop result for the vertex:

$$\begin{aligned} \Gamma_1^{\wedge\wedge\vee} &= \left(\Gamma_1^{\text{fermions}} + \Gamma_1^{\text{gluons}} + \Gamma_1^{\text{scalars}} \right)^{\wedge\wedge\vee} \\ &= -\frac{g^3}{4\pi^2} \frac{a}{m} \ln(1/a) \frac{p^+ K^\wedge}{p_1^+ p_2^+} \sum_{l=1}^{M_1-1} \left(\frac{2}{l} + \frac{1}{M_1-l} + \frac{1}{M-l} + \frac{F(l/M)}{M} \right) - (1 \leftrightarrow 2). \end{aligned} \quad (87)$$

Because of how loops are treated in the BT-worldsheet formalism it is natural to combine the one loop vertex result and the wave function renormalization for each fixed position of the solid line representing the loop. In other words we renormalize *locally* on the worldsheet. To clarify this, note the three different ways to insert a one loop correction to the cubic vertex at fixed l on the worldsheet, as in Fig. 18. Notice that the first and

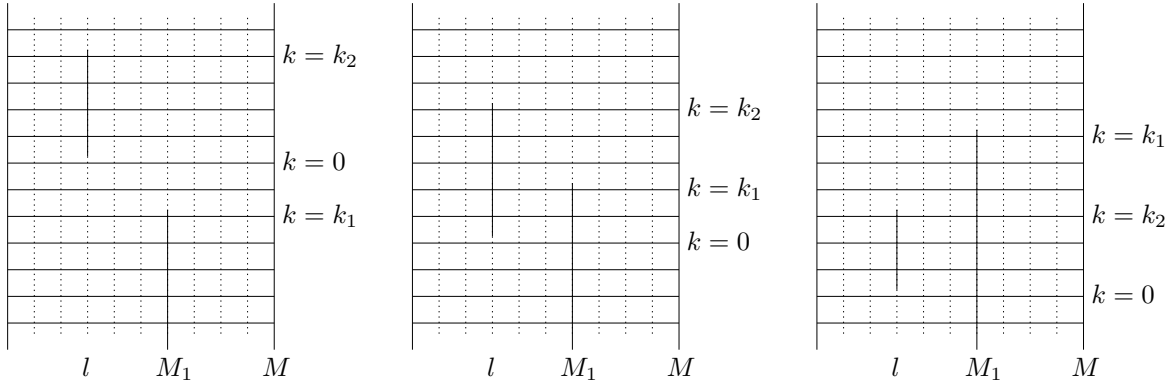


Figure 18: One loop diagrams for fixed l in the BT worldsheet picture.

last figures correspond to self energy diagrams for the legs with momenta (\mathbf{p}, M) and (\mathbf{p}_1, M_1) respectively. However, the middle figure corresponds to a triangle diagram with time ordering $k_1 > 0$. So combining our previous results we obtain for the Y 's corresponding to this polarization for each fixed $l < M_1$:

$$\begin{aligned} Y_l^{\wedge\wedge\vee} &= \Gamma_{1,l}^{\wedge\wedge\vee} + \frac{1}{2} \left(-2g \frac{a}{m} \frac{p^+ K^\wedge}{p_1^+ p_2^+} \right) (Z_l(M) - 1 + Z_l(M_1) - 1) \\ &= -\frac{g^3}{4\pi^2} \frac{a}{m} \ln(1/a) \frac{p^+ K^\wedge}{p_1^+ p_2^+} \left(\frac{2}{l} + \frac{1}{M_1-l} + \frac{1}{M-l} + \frac{F(l/M)}{M} \right) \\ &\quad + \frac{1}{2} \left(-2g \frac{a}{m} \frac{p^+ K^\wedge}{p_1^+ p_2^+} \right) \left(-\frac{g^2}{8\pi^2} \ln(1/a) \left\{ \frac{2}{l} + \frac{2}{M-l} + \frac{F(l/M)}{M} \right\} \right) \end{aligned}$$

$$\begin{aligned}
& -\frac{g^2}{8\pi^2} \ln(1/a) \left\{ \frac{2}{l} + \frac{2}{M_1 - l} + \frac{F(l/M_1)}{M_1} \right\} \\
= & -\frac{g^3}{8\pi^2} \frac{a}{m} \ln(1/a) \frac{p^+ K^\wedge}{p_1^+ p_2^+} \left(\frac{F(l/M)}{M} - \frac{F(l/M_1)}{M_1} \right). \tag{88}
\end{aligned}$$

We see that the terms of the form $1/l$, $1/(M_1 - l)$ and $1/(M - l)$ cancel in the final expression for Y . These terms multiply the $\ln(1/a)$ factor and would result in $\ln(1/m)$ factors if the sum is taken before Γ and \sqrt{Z} are combined. They represent the entanglement of $m \rightarrow 0$ with $a \rightarrow 0$ divergences and we have seen how this entanglement of divergences disappears locally on the worldsheet.

Finally, for completeness we present the analogous results for the triangle diagram with general polarization. The entangled divergence does not depend on the polarization of the external gluons. The local disentanglement discussed above therefore goes through unchanged for all polarizations. We write out the results for the renormalized vertex Y where a subscript \pm refers to the two different time orderings, $k_1 > 0$, ($l < M_1$) or $k_1 < 0$, ($l > M_1$) respectively.

$$Y_{\pm}^{\wedge\wedge} = Y_{\pm}^{\vee\vee} = 0, \tag{89}$$

$$Y_+^{\wedge\vee} = -\frac{g^3}{8\pi^2} \frac{a}{m} \ln(1/a) \frac{p^+ K^\wedge}{p_1^+ p_2^+} \sum_{l=1}^{M_1-1} \left(\frac{F(l/M)}{M} - \frac{F(l/M_1)}{M_1} \right), \tag{90}$$

$$Y_+^{\vee\wedge} = -\frac{g^3}{8\pi^2} \frac{a}{m} \ln(1/a) \frac{p_2^+ K^\wedge}{p_1^+ p^+} \sum_{l=1}^{M_1-1} \left(-\frac{F(l/M)}{M} - \frac{F(l/M_1)}{M_1} \right), \tag{91}$$

$$Y_+^{\vee\vee} = -\frac{g^3}{8\pi^2} \frac{a}{m} \ln(1/a) \frac{p_1^+ K^\wedge}{p_2^+ p^+} \sum_{l=1}^{M_1-1} \left(\frac{F(l/M_1)}{M_1} - \frac{F(l/M)}{M} \right), \tag{92}$$

$$Y_-^{\wedge\vee} = -\frac{g^3}{8\pi^2} \frac{a}{m} \ln(1/a) \frac{p^+ K^\wedge}{p_1^+ p_2^+} \sum_{l=M_1+1}^{M-1} \left(\frac{F(l/M)}{M} - \frac{F((l-M_1)/M_2)}{M_2} \right), \tag{93}$$

$$Y_-^{\vee\wedge} = -\frac{g^3}{8\pi^2} \frac{a}{m} \ln(1/a) \frac{p_2^+ K^\wedge}{p_1^+ p^+} \sum_{l=M_1+1}^{M-1} \left(\frac{F((l-M_1)/M_2)}{M_2} - \frac{F(l/M)}{M} \right), \tag{94}$$

$$Y_-^{\vee\vee} = -\frac{g^3}{8\pi^2} \frac{a}{m} \ln(1/a) \frac{p_1^+ K^\wedge}{p_2^+ p^+} \sum_{l=M_1+1}^{M-1} \left(-\frac{F(l/M)}{M} - \frac{F((l-M_1)/M_2)}{M_2} \right). \tag{95}$$

The expressions for the Y 's with $\wedge, \vee \rightarrow \vee, \wedge$ are obtained by the replacement $K^\wedge \rightarrow K^\vee$. We stress that the summands in the above expressions for Y are exactly the contributions of the three diagrams in Fig. 18 with the loop fixed at l .

Define the coupling renormalization $\Delta(N_f, N_f)$ by:

$$Y^{n_1 n_2 n_3} = Y_+^{n_1 n_2 n_3} + Y_-^{n_1 n_2 n_3} = \Gamma_0^{n_1 n_2 n_3} \Delta(N_f, N_s). \tag{96}$$

We then have in the limit $M_i \rightarrow +\infty$:

$$\Delta(N_f, N_s) = \frac{g^2}{8\pi^2} \ln(1/a) \left(\frac{11}{3} - \frac{N_f}{3} - \frac{N_s}{6} \right), \tag{97}$$

which is the well known result. In particular we have asymptotic freedom when $\Delta > 0$, and Δ vanishes for the particle content of $\mathcal{N} = 4$ supersymmetric Yang-Mills theory, $N_f = 8$ and $N_s = 6$.

For some cases such as the supersymmetric ($N_f = 2 + N_s$) or pure Yang-Mills ($N_f = N_s = 0$) the summands in the expressions for the Y 's do not change sign over their respective ranges. When $N_f < 8$, so that these cases are asymptotically free, the summands on the right sides of (92) and (94) have a sign which works against asymptotic freedom. Since the full sum exhibits asymptotic freedom for each polarization, this means that the complementary time orderings, (91) and (95), must contribute more than their share to asymptotic freedom. This fact may be useful for approximations involving selective graph summation.

7 Discussion and Concluding Remarks

In this article we have completed the “constructive” part of the Bardakci-Thorn program to cast the Feynman diagrams of quantum field theory in the language of string theory. That is, we have successfully extended the formalism to cover the full range of interesting supersymmetric gauge theories.

By construction our worldsheet systems exactly reproduce planar light-cone diagrams modulo issues associated with renormalization and the associated counter-terms necessary to cancel violations of Lorentz invariance that arise because the divergences of quantum field theory can amplify regulator artifacts, and we are working in a non-covariant gauge. In Section 6 we analyzed renormalization to one-loop order and confirmed that the necessary counter-term can be specified *locally* on the worldsheet. After that, the correct renormalization of coupling was obtained. Further, it was found that the renormalization behavior has an interesting local interpretation on the worldsheet. From a purely formal point of view the major issue left unresolved in this article is how Lorentz invariance and the renormalization program works on the worldsheet at 2 and higher loops. These questions are currently under active investigation.

An exciting aspect of the BT program is its potential application to the confinement problem of QCD. One of the biggest challenges in this regard is to have a model of confinement that simultaneously and systematically incorporates the perturbative short distance properties of QCD. This goal is the principal motivation for gluon chain model of confinement proposed in [8]. The BT worldsheet is an ideal setting for the construction of such models since its foundations rest explicitly on summing Feynman diagrams. The mean field method developed in [7] is a first step toward understanding the nonperturbative physics inherent in the BT worldsheet.

But the results of the present article set the stage more for a better understanding of Maldacena duality. Indeed, since our worldsheet construction succeeds for $\mathcal{N} = 4$ supersymmetric Yang-Mills theory, we now have a stringy description of the *weak* ’t Hooft coupling limit to complement the strong coupling description of IIB string theory on an $\text{AdS}_5 \times \text{S}_5$ manifold. So we can approach the weak coupling/strong coupling duality as a relation between two stringy descriptions rather than one between stringy and field theory descriptions. Perhaps it will be easier to probe the interpolation between weak and strong coupling in Maldacena duality since one can now seek a relation of apples to apples rather than apples to oranges. Features of perturbative QCD such as the scaling behavior of deep inelastic structure functions (or the anomalous dimensions of composite operators) can now be directly translated into the worldsheet formalism and then given a stringy interpretation. It will be interesting to compare this interpretation to that given by Gubser, Klebanov, and Polyakov in [19].

Acknowledgements. We would like to thank Zongan Qiu for helpful discussions in the early stages of this research. This work was supported in part by the Department of Energy under Grant No. DE-FG02-97ER-41029.

A Dirac Matrices

The Dirac matrices Γ^μ for the D dimensional Lorentz group are $2^{D/2} \times 2^{D/2}$ matrices with Γ^0 hermitian and Γ^i anti-hermitian, satisfying the Clifford algebra $\{\Gamma^\mu, \Gamma^\nu\} = -2\eta^{\mu\nu}$ with $\eta^{\mu\nu} = \text{diag}\{-1, 1, \dots, 1\}$. A spinor ψ transforms under the Lorentz group by $\delta\psi = -i\epsilon\Sigma^{\mu\nu}\psi/2$, and the conjugate spinor $\bar{\psi}$ by $\delta\bar{\psi} = +i\epsilon\bar{\psi}\Sigma^{\mu\nu}/2$. Here $\Sigma^{\mu\nu} = \frac{i}{2}[\Gamma^\mu, \Gamma^\nu]$.

We choose a representation for the Γ matrices that is particularly convenient for light-cone coordinates (see [18]). Picking the light-like directions $x^\pm = (x^0 \pm x^{D-1})/\sqrt{2}$, we fix Γ^0 and Γ^{D-1} to be

$$\Gamma^0 = i \begin{pmatrix} 0 & -I \\ I & 0 \end{pmatrix}, \quad \Gamma^{D-1} = i \begin{pmatrix} 0 & 0 & \mathbf{1} & 0 \\ 0 & 0 & 0 & -\mathbf{1} \\ \mathbf{1} & 0 & 0 & 0 \\ 0 & -\mathbf{1} & 0 & 0 \end{pmatrix}, \quad (98)$$

where I is the $2^{(D-2)/2}$ dimensional identity matrix, and $\mathbf{1}$ is the $2^{(D-4)/2}$ dimensional identity matrix. This will simplify the super-algebra in light-cone coordinates, singled out by the spatial component $D - 1$, since

$\alpha^{(D-1)}$ is diagonal:

$$\alpha^{(D-1)} \equiv \Gamma^0 \Gamma^{D-1} = \begin{pmatrix} \mathbf{1} & 0 & 0 & 0 \\ 0 & -\mathbf{1} & 0 & 0 \\ 0 & 0 & -\mathbf{1} & 0 \\ 0 & 0 & 0 & \mathbf{1} \end{pmatrix}. \quad (99)$$

The choice of representation for the transverse Γ^k , $k = 1, \dots, D-2$ can vary from one dimension to another depending on whether or not one applies Majorana or Weyl constraints (or both). We first separate the spinor components into two groups denoted by checked and unchecked lower case Latin spinor indices, according to the eigenvalues of the matrix α^{D-1} (99), the chirality matrix for $SO(1, 1)$:

$$\alpha_{\check{a}\check{b}}^{D-1} = -\delta_{\check{a}\check{b}} \quad (100)$$

$$\alpha_{a\check{b}}^{D-1} = \delta_{a\check{b}} \quad (101)$$

$$\alpha_{a\check{a}}^{D-1} = \alpha_{\check{a}\check{a}}^{D-1} = 0. \quad (102)$$

The checked and unchecked indices each range over $2^{(D-2)/2}$ values (16 for $D = 10$, 4 for $D = 6$, and 2 for $D = 4$). Because the transverse Γ^k commute with α^{D-1} , it follows that $\Gamma_{\check{a}\check{b}}^k = \Gamma_{a\check{b}}^k = 0$. On the light-cone, the checked components of the spinor fields are eliminated, leaving $2^{(D-2)/2}$ dimensional spinors ψ^a acted on by $O(D-2)$ Dirac matrices $\gamma_{ab}^k \equiv i\Gamma_{ab}^k$. by including the extra i in the definition of γ^k , we have rendered them hermitian and their Clifford algebra is $\{\gamma^k, \gamma^l\} = 2\delta_{kl}$.

To realize supersymmetric gauge theories in various dimensions we usually have to restrict the spinors to be Majorana ($D = 4$), Weyl ($D=4,6$), or Majorana-Weyl ($D=10$), so that the number of fermions equals the number of gauge bosons. Because we have chosen Γ^0 and Γ^{D-1} pure imaginary, and because our light-cone reduction picks the $+1$ eigenspace of $\Gamma^0 \Gamma^{D-1}$, these restrictions translate directly to corresponding restrictions on the γ_k . The Majorana representation, possible for $D = 2, 4 \pmod{8}$ specifies the γ_k to be real (and therefore symmetric). A Weyl friendly representation possible for D even is one for which the chirality matrix Γ_{D+1} is diagonal, and hence the same for the $O(D-2)$ chirality γ_{D-1} :

$$\gamma_{D-1} = \begin{pmatrix} \mathbf{1} & 0 \\ 0 & -\mathbf{1} \end{pmatrix}. \quad (103)$$

Imposing the Weyl constraint by fixing the chirality of a spinor to be ± 1 means keeping only the first (last) $2^{(D-4)/2}$ components. Only if $D = 2 \pmod{8}$ is the Majorana condition possible within the Weyl-friendly representation just described. The Majorana representation is also possible for $D = 4 \pmod{8}$, but then γ_{D-1} won't be diagonal. For example, in the case $D = 4$, a Majorana representation for the $O(D-2)$ gamma matrices can be taken to be

$$\gamma^1 = \sigma_1, \quad \gamma^2 = \sigma_3, \quad \text{with } \gamma_3 = -i\gamma^1\gamma^2 = -\sigma_2. \quad (104)$$

The Weyl-friendly representation for $D = 4$ would be

$$\gamma^1 = \sigma_1, \quad \gamma^2 = \sigma_2, \quad \text{with } \gamma_3 = -i\gamma^1\gamma^2 = \sigma_3. \quad (105)$$

B Details of One Loop Calculations

We consider the diagram depicted in Fig. 17 with fermions on internal lines and gluons with polarizations n_1, n_2 and n_3 on external lines. Using the fermion vertices from section 3 we get:

$$\sum_{l=1}^{M_1-1} \sum_{k_1, k_2} \int \frac{d\mathbf{q}}{(2\pi)^3} \exp \left\{ -\frac{a}{2m} \left(\frac{k_1(\mathbf{p}_1 - \mathbf{q})^2}{M_1 - l} + \frac{k_2 \mathbf{q}^2}{l} + \frac{(k_2 - k_1)(\mathbf{p} - \mathbf{q})^2}{M - l} \right) \right\} \\ \text{Tr} \left\{ \left[\frac{ag}{2m} (\gamma^{n_1} \gamma^r) \left(\frac{q}{l} - \frac{p_1 - q}{M_1 - l} \right)^r + \frac{ag}{m} \left(\frac{p_1 - q}{M_1 - l} - \frac{p_1}{M_1} \right)^{n_1} \right] \right\}$$

$$\left[\frac{ag}{2m} (\gamma^{n_3} \gamma^s) \left(\frac{p-q}{M-l} - \frac{q}{l} \right)^s + \frac{ag}{m} \left(\frac{q}{l} - \frac{p}{M} \right)^{n_3} \right] \left[\frac{ag}{2m} (\gamma^{n_2} \gamma^t) \left(\frac{p_1-q}{M_1-l} - \frac{p-q}{M-l} \right)^t + \frac{ag}{m} \left(\frac{p-q}{M-l} - \frac{p_2}{M_2} \right)^{n_2} \right]. \quad (106)$$

Notice that this is the expression associated with fermion arrows running counterclockwise around the loop. The other diagram contributes the same amount as this one. Also, this expression is for $k_1 > 0$, the other time ordering $k_1 < 0$ is obtained by making the substitution $p_1 \leftrightarrow p_2$ as in the gluon calculation of [17]. We now proceed much as in that calculation by completing the square in the exponent of Eq. (106) and shifting momentum:

$$\sum_{l=1}^{M_1-1} \sum_{k_1, k_2} \int \frac{d\mathbf{q}}{(2\pi)^3} \exp \left\{ -\frac{t_1+t_2+t_3}{2m/a} \mathbf{q}^2 \right\} e^{-H} \text{Tr} \left\{ \left[-\frac{g}{2} (\gamma^{n_1} \gamma^r) \frac{\chi_1^r}{l(M_1-l)} + g \frac{\chi_1^{n_1}}{M_1(M_1-l)} \right] \left[-\frac{g}{2} (\gamma^{n_3} \gamma^s) \frac{\chi_3^s}{l(M-l)} + g \frac{\chi_3^{n_3}}{Ml} \right] \left[\frac{g}{2} (\gamma^{n_2} \gamma^t) \frac{\chi_2^t}{(M_1-l)(M-l)} + g \frac{\chi_2^{n_2}}{(M-l)M_2} \right] \right\}, \quad (107)$$

with

$$\chi_1^n = \frac{t_3 K^n / m}{t_1 + t_2 + t_3} - M_1 q^n, \quad \chi_2^n = \frac{t_2 K^n / m}{t_1 + t_2 + t_3} - M_2 q^n, \quad \chi_3^n = \frac{t_1 K^n / m}{t_1 + t_2 + t_3} + M q^n, \quad (108)$$

$$t_1 = \frac{k_1}{M_1 - l}, \quad t_2 = \frac{k_2}{l}, \quad t_3 = \frac{k_2 - k_1}{M - l}, \quad (109)$$

$$H = \frac{a}{2m} \frac{t_1 t_3 \mathbf{p}_2^2 + t_1 t_2 \mathbf{p}_1^2 + t_2 t_3 \mathbf{p}^2}{t_1 + t_2 + t_3}. \quad (110)$$

In the \mathbf{q} -integral only the terms proportional to \mathbf{q}^2 times the Gaussian will exhibit $a \rightarrow 0$ divergences so we retain only those. The general loop integral is given by:

$$\int d\mathbf{q} \chi_1^i \chi_3^k \chi_2^j \exp \left\{ -\frac{t_1+t_2+t_3}{2m/a} \mathbf{q}^2 \right\} \rightarrow \frac{(2m/a)^2 \pi}{2(t_1+t_2+t_3)^3} (M_1 M_2 t_1 (K^k/m) \delta^{ij} - M_1 M t_2 (K^j/m) \delta^{ik} - M_2 M t_3 (K^i/m) \delta^{jk}). \quad (111)$$

(The arrow means that $a \rightarrow 0$ finite terms have been dropped.) Some simplification can be done right away, for example the term proportional to $\text{Tr}(\gamma^{n_1} \gamma^r \gamma^{n_3} \gamma^s \gamma^{n_2} \gamma^t)$ after contracting with the momentum integral is proportional to:

$$\sum_r \text{Tr}(\gamma^{n_1} \gamma^r \gamma^{n_3} \gamma^r \gamma^{n_2} (\boldsymbol{\gamma} \cdot \mathbf{K})) = (4 - D_0) \text{Tr}(\gamma^{n_1} \gamma^{n_3} \gamma^{n_2} (\boldsymbol{\gamma} \cdot \mathbf{K})), \quad (112)$$

where D_0 is the spacetime dimensionality of the loop momentum integral, that is the reduced dimension $D_0 = 4$ so this term vanishes. Further simplifications can be seen when a particular external polarization is chosen.

The detailed $a \rightarrow 0$ behavior becomes apparent when the sum over k_1 and k_2 is done. With a little work it can be shown that:

$$\sum_{k_1, k_2} \frac{t_1}{(t_1+t_2+t_3)^2} e^{-H} \rightarrow \ln(1/a) \frac{l^3 (M-l)(M_1-l)}{2M_1^2 M}, \quad (113)$$

$$\sum_{k_1, k_2} \frac{t_2}{(t_1+t_2+t_3)^2} e^{-H} \rightarrow \ln(1/a) \frac{l^2 (M-l)(M_1-l)}{2M_1 M} \left(\frac{M_1-l}{M_1} + \frac{M-l}{M} \right), \quad (114)$$

$$\sum_{k_1, k_2} \frac{t_3}{(t_1+t_2+t_3)^2} e^{-H} \rightarrow \ln(1/a) \frac{l^3 (M-l)(M_1-l)}{2M_1 M^2}. \quad (115)$$

Carrying this through for the polarization $n_1 = n_2 = n_3 = n$ yields:

$$\frac{N_f a g^3 (K^n/m)}{32\pi^2 m} \frac{\ln(1/a)}{M_1 M_2 M} \sum_{l=1}^{M_1-1} \left\{ M \left[1 - 2 \frac{l}{M} \left(1 - \frac{l}{M} \right) \right] + M_1 \left[1 - 2 \frac{l}{M_1} \left(1 - \frac{l}{M_1} \right) \right] \right\}. \quad (116)$$

In the continuum limit we have $\sum_{l=1}^{M_i-1} f(l/M_j) \rightarrow M_j \int_0^{M_i/M_j} dx f(x)$ for any continuous function f . Therefore, after adding the $k_1 < 0$ contribution and multiplying by 2 for the other orientation of the fermion loop we obtain:

$$\frac{N_f g^3}{16\pi^2} K^n \frac{a}{m} \frac{(p_1^+)^2 + (p_2^+)^2 + (p^+)^2}{p_1^+ p_2^+ p^+} \ln(1/a) \frac{2}{3}. \quad (117)$$

In contrast, the calculation and result for the $n_1 = n_2 = \wedge, n_3 = \vee$ polarization is a lot simpler. The expression analogous to (116) is:

$$-\frac{N_f g^3}{16\pi^2} \frac{a}{m} \ln(1/a) \frac{p^+ K^\wedge}{p_1^+ p_2^+} \sum_{l=1}^{M_1-1} \frac{1}{M} \left[1 - 2 \frac{l}{M} \left(1 - \frac{l}{M} \right) \right]. \quad (118)$$

The result shown in (82) is obtained from this one by adding the $k_1 < 0$ contribution and multiplying by two which accounts for the other orientation of the fermion arrows in the loop.

References

- [1] K. Bardakci and C. B. Thorn, Nucl. Phys. B **626** (2002) 287 [arXiv:hep-th/0110301].
- [2] G. 't Hooft, Nucl. Phys. **B72** (1974) 461.
- [3] P. Goddard, J. Goldstone, C. Rebbi, and C. B. Thorn, Nucl. Phys. **B56** (1973) 109.
- [4] S. Mandelstam, Nucl. Phys. **B64** (1973) 205; Phys. Lett. **46B** (1973) 447; Nucl. Phys. **B69** (1974) 77; see also his lectures in *Unified String Theories*, ed. M. Green and D. Gross (World Scientific) 1986.
- [5] R. Giles and C. B. Thorn, Phys. Rev. **D16** (1977) 366.
- [6] C. B. Thorn, Nucl. Phys. B **637** (2002) 272 [arXiv:hep-th/0203167].
- [7] K. Bardakci and C. B. Thorn, arXiv:hep-th/0206205.
- [8] J. Greensite and C. B. Thorn, JHEP **0202** (2002) 014 [arXiv:hep-ph/0112326].
- [9] G. 't Hooft, arXiv:hep-th/0207179.
- [10] J. M. Maldacena, Adv. Theor. Math. Phys. **2** (1998) 231-252, hep-th/9711200.
- [11] E. Witten, Adv. Theor. Math. Phys. **2** (1998) 253-291 hep-th/9802150.
- [12] S. S. Gubser, I. R. Klebanov, and A. M. Polyakov, Phys. Lett. **B428** (1998) 105, hep-th/9802109.
- [13] H. Nastase and W. Siegel, JHEP, 0010:040 (2000), hep-th/0010106.
- [14] D. Berenstein, J. M. Maldacena and H. Nastase, JHEP **0204** (2002) 013 [arXiv:hep-th/0202021].
- [15] K. Bering, J. S. Rozowsky and C. B. Thorn, Phys. Rev. **D61** (2000) 045007, hep-th/9909141.
- [16] C. B. Thorn, Phys. Rev. **D20** (1979) 1934.
- [17] S. Gudmundsson and C. B. Thorn, arXiv:hep-th/0203232.
- [18] O. Bergman and C. B. Thorn, Phys. Rev. **D52** (1995) 5980.
- [19] S. S. Gubser, I. R. Klebanov and A. M. Polyakov, Nucl. Phys. B **636** (2002) 99 [arXiv:hep-th/0204051].